DIRECT SPECTRA-TO-SPECTRA METHODS

REPORT 2024:1030

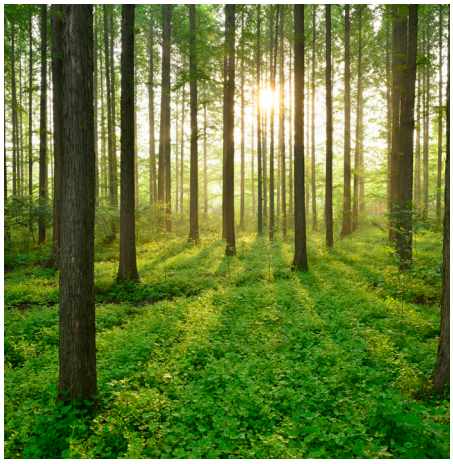

NUCLEAR POWER CONCRETE TECHNOLOGY

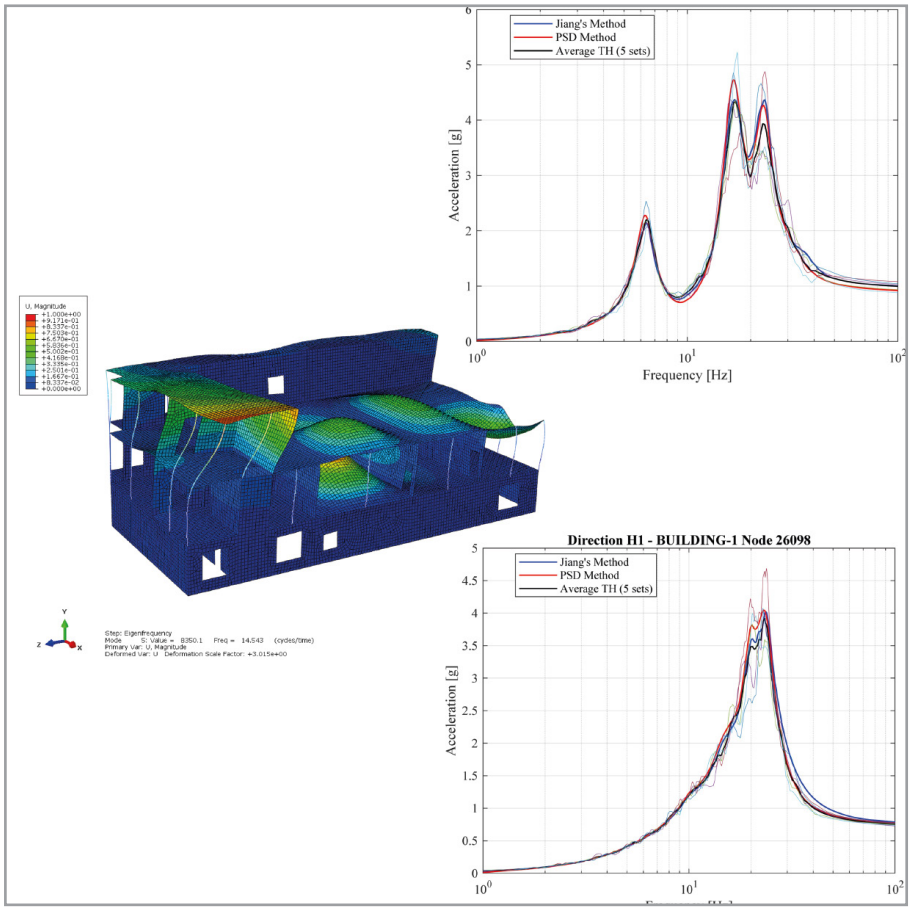

Energiforsk

Direct Spectra-to-Spectra Methods

Alternative Methods for Development of Floor Response Spectra at Nuclear Facilities in Sweden and Finland

DANIEL RYDLE, MARTIN OLOFSSON, ALBIN BÄCKSTRAND
MICHELE GODIO, GABRIEL BARSLIVO

ISBN 978-91-89919-30-3 | © Energiforsk July 2024

Energiforsk AB | Phone: 08-677 25 30 | E-mail: kontakt@energiforsk.se | www.energiforsk.se

Foreword

The Energiforsk Nuclear Power Concrete Program aims to increase the knowledge of aspects affecting safety, maintenance and development of concrete structures in the Nordic nuclear power plants. A part of this is to investigate possibilities to facilitate and simplify the work that is performed in the nuclear business.

Safety-related structures, systems, and components must undergo verification for loads following earthquake events, as mandated by the current regulations and applicable codes. The methods used today in the Nordics are complex, requiring large data models and extensive data input.

This study aims to investigate the possibility of simplifying the work whilst safeguarding quality and reliability, by using so-called Direct Spectra-to-Spectra Methods. Furthermore, the work aims to disseminate knowledge about these methods in the Nordics and highlight their benefits and potential limitations.

The study shows that the two investigated Direct Spectra-to-Spectra Methods can be concluded to perform well in comparison to the more well-established time series method and are judged adequate to use in various design situations.

The study was carried out by Daniel Rydle and Gabriel Barslivo, Vattenfall; and Martin Olofsson, Albin Bäckstrand and Michele Godio, Rise. The study was performed within the Energiforsk Nuclear Power Concrete Program which is financed by Vattenfall, Uniper, Fortum, TVO, Skellefteå Kraft, Karlstads Energi, SSM and SKB.

These are the results and conclusions of a project, which is part of a research programme run by Energiforsk. The author/authors are responsible for the content.

Summary

Structural verification of Structures, Systems, and Components (SSC) mounted in nuclear power plants (NPP) and auxiliary buildings is of paramount importance for safety. At both Swedish and Finnish NPPs, safety-related SSCs must undergo verification for loads following earthquake events as mandated by the current regulations and applicable codes. Typically, the structural verification of these systems relies on input data of the loading in the form of Floor Response Spectra (FRS), which are derived from earthquake analyses of the buildings. In Sweden and Finland, the development of FRS is normally performed based on time history analysis according to the recommendations given in ASCE 4-98 [1] or its successor ASCE 4-16 [2]. However, the computational cost when using time history analysis can be significant, particularly for large models. Furthermore, ASCE 4-16 requires the use of at least five independent sets of acceleration time series. To address these challenges, alternative approaches known as Direct Spectra-to-Spectra Methods (DSSM) have been developed. These methods, which are based on eigenfrequency analysis of the structures, offer a more computationally efficient solution compared to time history analysis. ASCE 4-16 recognizes the efficacy of DSSMs, particularly those grounded in a theoretical framework based on random vibrations. In the commentary part of ASCE 4-16, several DSSMs from the literature are recommended. Despite the potential benefits of DSSMs, their application in Sweden and Finland for development of FRS remains limited.

The primary purpose of this study is to investigate the possibility of utilizing DSSMs for the development of FRS at Swedish and Finnish nuclear facilities. Furthermore, the work aims to disseminate knowledge about these methods in the two countries, and highlight their benefits and potential limitations. The aim of the work is also to develop a library of MATLAB scripts, and share the library along with this report.

Based on the findings of a literature survey, two DSSMs were selected for implementation in MATLAB and further evaluation. The two selected DSSMs include a recent method developed by Jiang et al. [3] [4] [5], and a method that explicitly utilizes equivalent Power Spectral Density functions (PSD) of the design Ground Response Spectra (GRS) together with the work reported by Lalanne [6] [7]. The performance of the two methods was evaluated using two example structures, one representing a simplified containment structure and, the other, a generic service building with closely spaced modes. In the evaluation, the FRS obtained using the two selected DSSMs are compared to the FRS generated by time history analyses in accordance with ASCE 4-16.

The FRS obtained using the three different methods show an overall good agreement in shape and acceleration response at the peaks. The obtained results also show that there is a significant scatter at the peaks between the individual FRS generated by the time history analyses. This highlights the importance of using several sets of acceleration time series followed by averaging of the results when using this method, as is also stipulated by ASCE 4-16. However, the FRS obtained using either of the two DSSMs mainly falls within the scatter of the time-history

based FRS. The two DSSMs investigated in this study can thus be concluded to perform well in comparison to the more well-established time series method for the evaluation of FRS, and are judged adequate to use in various design situations. Additionally, it can be concluded that the required computational time is significantly reduced through the use of DSSMs. In both examples, the analysis time for the time history analyses was roughly 200 times longer than in the eigenfrequency analyses. The use of DSSMs can thus help significantly speed-up the seismic design of SCCs. This is particularly true in preliminary design stages, where the analyst needs to investigate several different design alternatives.

Keywords

Earthquakes, Direct Spectra-to-Spectra, Power Spectral Density (PSD), Floor Response Spectra, In-structure Response Spectra, Secondary Response Spectra, Finite Element Analysis, MATLAB Scripts

Sammanfattning

Strukturell verifiering av konstruktioner, system och komponenter (SSC) som finns monterade i kärnkraftverk och omkringliggande byggnader är av yttersta vikt för säkerheten. Vid både svenska och finska kärnkraftverk måste säkerhetsrelaterade SSC verifieras för de laster som följer av en jordbävning i enlighet med gällande regelverk och designkoder. Lasterna för verifiering av dessa system erhålls vanligen i form av golvresponsspektra (FRS), vilka utvärderats från jordbävnings-analyser av byggnaderna. I Sverige och Finland utvärderas golvresponsspektra normalt från tidshistorieanalyser som utförts i enlighet med de rekommendationer som ges i ASCE 4-98 [1] eller dess efterföljare ASCE 4-16 [2]. Tidshistorieanalyser kan dock i många fall bli beräkningstunga, särskilt för stora modeller. I tillägg bör nämnas att ASCE 4-16 dessutom föreskriver att minst fem set av oberoende tidshistorier för accelerationerna ska användas vid denna typ av analys. För att avhjälpa dessa nackdelar med tidshistorieanalyser har alternativa metoder benämnda direkt spektra-till-spektra-metoder (DSSM) utvecklats. Dessa direktmetoder bygger istället på egenfrekvensanalys av strukturerna, varför en mer beräkningseffektiv lösning kan erhållas i jämförelse med tidshistorieanalys. I ASCE 4-16 omnämns även möjligheten att använd direktmetoder, och då särskilt de direktmetoder som grundar sig i ett teoretiskt ramverk baserat på slumpmässiga vibrationer. I kommentarsdelen av ASCE 4-16 rekommenderas ett flertal olika direktmetoder som finns publicerade i litteraturen. Trots de potentiella fördelar som finns med direktmetoder är tillämpningen av dessa metoder för beräkning av golvresponsspektra begränsad i både Sverige och Finland.

Det huvudsakliga syftet med föreliggande studie är att utreda möjligheten att använda direktmetoder för utvärdering av golvresponsspektra vid svenska och finska kärntekniska anläggningar. Vidare syftar arbete till att sprida kunskap om dessa metoder i de två länderna samt belysa deras fördelar och potentiella begränsningar. Målet är också att utveckla ett bibliotek med MATLAB-skript, samt att sprida detta bibliotek tillsammans med rapporten.

Baserat på resultatet av en inledande litteraturstudie valdes två olika direkt-metoder ut för implementering i MATLAB och vidare utvärdering. De två valda direktmetoderna inkluderar en nyligen utvecklad metod av Jiang et al. [3] [4] [5], samt en metod som explicit nyttjar ekvivalenta effektspektra (PSD) av jordbävningens markresponsspektra i kombination med de samband som togs fram av Lalanne [6] [7]. Utvärderingen av metoderna genomfördes med hjälp av två exempel. I det första exemplet användes en förenklad modell av en reaktorinneslutning, och i det andra exemplet en modell av en generisk servicebyggnad med tätt liggande egenmoder. I utvärderingen jämfördes erhållna golvresponsspektra från de två utvalda direktmetoderna med golvresponsspektra beräknade från tidshistorieanalyser som utförts i enlighet med rekommendationerna i ASCE 4-16.

Erhållna golvresponsspektra från de tre använda metoderna visar överlag god överenstämmelse sett till form och accelerationsrespons kring pikarna. Vidare kan det i resultaten observeras en påtaglig spridning i respons mellan erhållna

golvresponsspektrum från de enskilda tidshistorieanalyserna kring pikarna. Detta understryker vikten av att använda flera set av accelerationstidshistorier följt av medelvärdesbildning av resultaten när denna metod används för utvärdering av golvresponsspektra, vilket också föreskrivs i ASCE 4-16. Det bör dock poängteras att erhållna golvresponsspektra med de två direktmetoderna huvudsakligen ligger inom spridningsintervallet för de golvresponsspektra som erhållits baserat på tidshistorieanalys. De två direktmetoderna som undersökts i denna studie kan således konstateras ge resultat som har god överensstämmelse med den mer väletablerade tidshistoriemetoden för utvärdering av golvresponsspektra. Direktmetoderna bedöms därför också möjliga att tillämpa i olika dimensioneringssituationer. I tillägg kan det också konstateras att det är möjligt att signifikant reducera beräkningstiden genom användning av direktmetoder. I de två presenterade exemplen var analystiden för tidshistorieanalyserna ungefär 200 gånger länger än i egenfrekvensanalyserna. Användning av direktmetoder kan därför i vissa situationer hjälpa till att avsevärt effektivisera seismisk design av SSC. Detta gäller särskilt i tidig design då ingenjören behöver undersöka ett flertal olika utformningsalternativ.

List of content

Abbreviations

ASCE	American Society of Civil Engineers
DOF	Degree of Freedom
DSSM	Direct Spectra-to-Spectra Method
FEM	Finite Element Method
FRS	Floor Response Spectrum/Spectra. Also commonly called In-Structure Response Spectra and Secondary Response Spectra
GRS	Ground Response Spectrum/Spectra
MDOF	Multiple Degrees of Freedom
NPP	Nuclear Power Plant
PSD	Power Spectral Density Function
SDOF	Single Degree of Freedom
SRSS	Square Root of Sum of the Squares
SSC	Structures, Systems, and Components
TH	Time History/Histories
THA	Time History Analysis/Analyses
tRS	Tuning Response Spectrum/Spectra

1 Introduction

1.1 BACKGROUND

Structural verification of Structures, Systems, and Components (SSC) mounted in nuclear power plants (NPP) and auxiliary buildings is of paramount importance for the safety. At both Swedish and Finnish NPPs, safety-related SSCs must undergo verification for loads following earthquake events as mandated by the current regulations and applicable codes. Typically, the seismic integrity verification of these systems relies on input data of the loading in the form of Floor Response Spectra (FRS), which are derived from earthquake analyses of the buildings. In Sweden and Finland, the development of FRS is normally performed based on time history analysis according to the recommendations given in ASCE 4-98 [1] or its successor ASCE 4-16 [2].

However, the computational cost when using time history analysis can be significant, particularly for large models. Furthermore, ASCE 4-16 requires the use of at least five independent sets of acceleration time series. To address these challenges, alternative approaches known as Direct Spectra-to-Spectra Methods (DSSM) have been developed. These methods, which are based on eigenfrequency analysis of the structures, offer a more computationally efficient solution compared to time history analysis. ASCE 4-16 recognizes the efficacy of DSSMs, particularly those grounded in a theoretical framework based on random vibrations. In the commentary part of ASCE 4-16, several DSSMs in the literature are recommended, e.g. the approach reported by Singh [8] [9] from the late 1970's. In more recent literature, the DSSM proposed by Jiang et al. [3] has been demonstrated to be effective for complex building structures with closely spaced eigenmodes. Jiang's method has also been further developed to account for soil-structure interaction (SSI) [10], evaluation of FRS in structures under seismic excitation at multiple supports [11] and for development of tertiary response spectra [12]. The latter term refers to response spectra of systems mounted on another system in a structure, e.g. a valve mounted on a piping system. Despite the potential benefits of DSSMs, their application in Sweden and Finland for FRS evaluation remains limited.

1.2 AIMS AND SCOPE

The primary purpose of this study is to investigate the possibility of utilizing DSSMs for evaluation of FRS at Swedish and Finnish nuclear facilities. Furthermore, the work aims to disseminate knowledge about these methods in the two countries and highlight their benefits and potential limitations. The aim of the work is also to develop a library of scripts for at least one of the studied DSSMs, and share the library together with this report.

1.3 METHOD

To achieve the purpose and goals of this study, the work has been structured into the following activities:

- Literature study: Investigation of various DSSMs proposed in the literature to identify suitable methods. This activity involves not only selecting the methods, but also describing their general structure and theoretical basis that they are founded on. The aim was to identify two suitable DSSMs for further evaluation.
- Implementation in computer code: Implementation of the two selected DSSMs in MATLAB. As mentioned in the previous section, a library of scripts is shared together with this report.
- Evaluation of DSSMs: Investigation of the performance of the selected DSSMs based on the Swedish earthquake at hard rock sites with an annual exceedance probability of 10^{-6}. The investigation includes two example structures: a simplified containment structure and a generic service building with closely spaced modes. FRS are developed and compared in selected locations of the structures using time history analysis and the chosen DSSMs. Based on the results from the examples, benefits and potential limitations of the methods are evaluated.

1.4 LIMITATIONS

Even though there are numerous DSSMs proposed in the literature, only two DSSMs were assessed in this study. The focus has been on more recent methods since these still are being developed through addition of new features to account for various important aspects.

In the evaluation of the DSSMs, only the Swedish earthquake at hard rock sites with an annual exceedance probability of 10^{-6} was considered. This earthquake was chosen since 5 independent sets of spectrum-compatible (and ASCE 4-98 compliant) acceleration time series already were available. Given the purpose of the study, this choice does, however, not significantly limit the conclusions that can be drawn from the results. Furthermore, the similarities in seismic characteristics between Sweden and Finland mean that the findings should also be applicable for Finnish conditions.

2 Direct spectra-to-spectra methods

2.1 LITERATURE SURVEY AND CHOICE OF METHODS

Secondary systems are integral components that are supported by the primary structure. In NPPs, secondary systems include safety-related equipment like electrical, mechanical, and control systems. Despite their name, these systems are crucial, as they maintain operational processes in the primary system, support human activities, and can often cost more than the main structure. For the above reasons, seismic analysis is required for the design and assessment of these secondary systems.

ASCE 4-16 [2] proposes both THAs and DSSMs for the generation of FRS. While the former method is straightforward as it can be conducted by modal superposition or direct time integration, it requires knowledge on the site-specific ground motions in time domain, which often can only be artificially reproduced. According to the definition used by Jiang [3], the latter consists in generating FRS directly from the GRS without generating any intermediate input such as spectrum-compatible time histories or power spectral density functions (PSDs). Instead, the FRS are being expressed as functions of the GRS and modal parameters of the primary structure.

Spectrum-to-spectrum methods in seismic analysis are built on the concept of response spectra. A response spectrum is a graphical representation that shows the maximum response, in terms of displacement, velocity, or acceleration, of a series of SDOF systems to a particular ground motion, plotted as a function of the frequency or period of said systems. In the practice, said tool is utilized to estimate how structures respond to seismic actions. A DSSM is meant to transform the GRS, representing the seismic input, directly into an FRS, which represents the response of the primary structure to that input at a certain location.

DSSMs involve several steps, starting with the characterization of the ground motion through the GRS. In direct methods, this spectrum is then used alongside the dynamic properties of the structure (mass, damping, and stiffness) to generate the final FRS. One key aspect of this method is the modal decomposition, which separates the response of a MDOF system into a series of SDOF systems. This simplification allows for the direct application of the input spectrum to each mode of vibration, followed by a recombination process to reconstruct the overall structural response.

Two practical methodologies can be used to determine the seismic responses of secondary systems: a coupled (or combined) primary-secondary system approach and a decoupled one.

Under the coupled primary-secondary system approach, the primary and secondary systems are modelled together. To this class belong both THAs and several DSSMs. By way of example for the latter, [13] [14] [15] developed a perturbation-technique-based modal analysis method to generate FRS of the combined system. However, despite being accurate on a theoretical basis, the coupled approach is not widely accepted in the practice [16]. In fact, challenges

may arise in modal or time history analyses due to large differences between the primary and secondary systems in characteristics such as mass and stiffness, which may finally lead to inaccurate numerical solutions. Moreover, the approach is considered impractical in handling various locations and a large number of secondary systems.

Since most secondary systems have relatively small mass compared to the mass of the supporting structure, the effect of interaction between the primary and secondary system is often negligible. This makes uncoupled FRS methods more widely accepted in the practice. Both THAs and DSSMs belong to the class of uncoupled approaches. Several criteria to select between coupled and decoupled approaches are recommended in [17] [18].

Research on uncoupled DSSM approaches has been conducted since the 70's. Biggs & Roesset [19] presented a semi-empirical technique for producing FRS without requiring THA. A probabilistic approach was incorporated into Singh's method [8] of generating FRS based on random vibration theory. Singh [9] expanded on this strategy by considering resonant situations, which occur when the frequency of the secondary system is near to that of the primary system. However, for structures with closely spaced vibration modes, this method did not prove suitable when the equipment was in resonance with several structural modes (tuning cases).

More recently, An et al. [20] developed a direct method to generate FRS estimates in the time domain rather than the frequency domain, by computing the Duhamel integral between unit impulse response functions. Calvi & Sullivan [21] proposed a way to predict acceleration spectra for the seismic design of secondary system supported by MDOF structures. In this method, an empirical relationship between dynamic amplification coefficients and elastic damping developed in [22] was utilized. Haymes et al. [23] further refined the method by Calvi & Sullivan by applying a modification to the amplification factor shape, which could then consider both floor acceleration and displacement response spectra. A modified equation for predicting the relative spectral displacements for periods longer than the effective periods of the supporting structures was also proposed by Merino et al. [24]. Vukobratović and Fajfar [25] [26] [27] developed a method for direct generation of FRS for MDOF structures based on the theory of structural dynamics and empirically determined amplification factors, providing an approximation of FRS when the structures are inelastic.

Another method that is worthwhile mentioning, which was also specifically developed for the seismic analysis of secondary systems supported by MDOF structures, is the one of Asfura & Der Kiureghian [28], who proposed a DSSM to evaluate the total displacement spectra. This was achieved by introducing the concept of "cross-oscillator, cross-floor response spectrum". However, this method appeared to be cumbersome for determining the forces in the members of the secondary system. To solve this problem, Burdisso & Singh [29] introduced the concept of pseudo-static response, dividing the response of the structure into a pseudo-static and dynamic part, which were later combined based on the theory of random vibration. Similarly, Saudy [30] proposed an alternative modal combination rule to improve its performance in cases of tuned combined primary-secondary systems.

Despite the existence of several DSSMs for generating FRS in the literature, only a few of them have been used for NPPs, showing conservative results in some frequency ranges and unconservative ones in others due to the various approximations being used [11], see e.g. Asfura and Der Kiureghian [28], An et al. [20], etc.

Recently, Jiang et al. [4] [3] developed a DSSM tailored for NPPs which resulted in two major novelties with respect to the methods proposed previously in the literature:

1) The concept of tRS, which was proposed to deal with the tuning cases. Statistical relationships between tRS and GRS were developed in a companion work [5] based on the results from simulations performed with a large number of real earthquake records.

2) A new combination rule called FRS-CQC (Floor Response Spectrum - Complete Quadratic Combination), derived from the theory of random vibration, accounting for not only the correlation between responses of structural modes but also correlations between responses of equipment and structural modes. Said rule was proven to be capable of dealing with structures with closely spaced modes.

Initially developed for structures built on rigid foundations, the DSSM proposed by Jiang et al. [4] has been extended to structures subjected to earthquake excitations at multiple supports [11], to account for soil-structure interaction (SSI) [10] and for development of tertiary response spectra [12]. The latter term refers to response spectra of systems mounted on another system in a structure, e.g. a valve mounted on a piping system.

In the present study, the method by Jiang et al. [4], henceforth shortly indicated as "Jiang's method", is implemented and tested versus THA along with another DSSM, inspired by the work of Lalanne [6] [7] and herein referred to as the "PSD method". The PSD method proposed here is based on the relation between a random process and its response spectrum. This method predicates on the idea that the peak response can only be meaningfully evaluated in a probabilistic context. It has been successfully implemented by the authors for another application, that is, the vibration analysis for relevant comparison of measured field vibration environment data with random vibration profiles for vibration endurance testing. The method builds on the intuition of Christian Lalanne, who developed a response spectrum method for that application in the late 70's and early 80's [6] [7]. The method gained little attention outside France before taking off roughly 20 years later. As stationary random vibration is often used in vibration endurance testing, Lalanne made use of the mathematical developments made in the 40's by S. O. Rice [31] and in the 60's by J. S. Bendat [32] for the estimation of extreme values in stationary random processes passing through dynamical systems. Explicit use of PSD functions for generation of FRS is not common in the literature. One approach is presented in, e.g., [33], but few details are provided, which prevents its understanding and implementation. However, the use of PSDs in the development of DSSMs is not a novelty. The theoretical basis of, e.g., Singh's [8] [9] approach relies on PSDs, but a number of simplifying assumptions are

introduced, which eliminates the explicit use of a PSD. Instead, a number of coefficients that lack physical meaning to engineers need to be determined by solving several systems of equations. Experience from the literature has shown that numerical difficulties may be encountered when solving these systems of equations for large complex structures [3].

Compared to the rather old DSSMs that are recommended in the commentary part of ASCE 4-16 (e.g. [8] [9]), the DSSMs that are chosen for assessment in this study are relatively recent, are still being developed through the addition of new features to account for other relevant practical aspects, and are best fit for modern computing power. Below, the foundations and main governing equations of the two above selected methods are briefly reported.

2.2 JIANG'S METHOD

In this section, the basic principles of the method developed by Jiang et al. [3] [4] [5] are briefly presented. The purpose is not to present a complete derivation of all expressions, but rather to highlight the major steps, including introduced assumptions and simplifications, and the obtained relationships relevant for implementation of the method in any computer code of choice. For the interested reader, a complete derivation of the method can be found in [3] and [4]. Note that the notations used in the two cited references are also adopted in this report.

The major principle in the development of Jiang's method was to initially derive analytical relationships for the FRS in time domain based on Duhamel's integral. In the first step of the derivation, relationships are derived for the motion of a SDOF oscillator mounted on a SDOF structure. The unit-impulse response functions in Duhamel's integral for the oscillator (h_0) and the structure (h) are defined adopting the following notations

$$h_0(t) = e^{-\zeta_0 \omega_0 t} \frac{\sin\left(\omega_{0,d} t\right)}{\omega_{0,d}}$$

$$h(t) = e^{-\zeta \omega t} \frac{\sin(\omega_d t)}{\omega_d}$$

$$\omega_{0,d} = \omega_0 \sqrt{1 - \zeta_0^2}$$

$$\omega_d = \omega \sqrt{1 - \zeta^2}$$

where the circular frequency and damping coefficient of the oscillator and the structure are denoted ω_0, ζ_0 and ω, ζ, respectively. Utilizing Duhamel's integral and assuming lightly-damped systems ($\zeta_0, \zeta < 0.2$), meaning that some second-order terms containing the damping are negligible, an expression for the maximum response of a oscillator mounted on a structure can be obtained

$$S_F(\omega_0, \zeta_0) = |\ddot{u}_F(t)|_{max} \approx \omega_0^2 \omega^2 \left| h_0(t) * h(t) * \ddot{u}_g(t) \right|_{max} \quad (2\text{-}1)$$

where $S_F(\omega_0, \zeta_0) = |\ddot{u}_F(t)|_{max}$ is the spectral acceleration of the SDOF oscillator, i.e.

its maximum acceleration response, and $\ddot{u}_g(t)$ is the ground acceleration. Note that the operator $*$ here denotes the convolution of two functions. If the SDOF oscillator is directly mounted on the ground, the term $\omega^2 h(t)$ can be removed, and the expression in Eq. (2-1) reduces to a corresponding GRS response value S_A according to

$$S_A(\omega_0, \zeta_0) = |\ddot{u}_F(t)|_{max} \approx \omega_0^2 \left| h_0(t) * \ddot{u}_g(t) \right|_{max}. \tag{2-2}$$

The expression in Eq. (2-1) for the spectral acceleration response of the oscillator is evaluated in time domain. To obtain a form of the expression that enables one to go directly from a GRS to a FRS, another solution to the equation must be sought. The first convolution term in Eq. (2-1), i.e. $h_0(t) * h(t) = C(t)$, describes the response of the oscillator under the excitation of $h(t)$ from the structure. Hence, from the equation of motion for a SDOF system, the following relationship must also hold

$$\ddot{C}(t) + 2\zeta_0\omega_0\dot{C}(t) + \omega_0^2 C(t) = h(t) = \frac{1}{\omega_d} e^{-\zeta\omega t} \sin(\omega_d t). \tag{2-3}$$

The general solution to the second order differential equation in Eq. (2-3) consists of a complementary solution $C_c(t)$ and a particular solution $C_p(t)$, which can be expressed on the following form

$$C(t) = C_c(t) + C_p(t). \tag{2-4}$$

In this case, the complementary solution can be written as

$$C_c(t) = e^{-\zeta_0\omega_0 t}[C_1 \cos(\omega_{0,d} t) + C_2 \sin(\omega_{0,d} t)] \tag{2-5}$$

where C_1 and C_2 are two coefficients given by the initial conditions of the oscillator. Initially, the non-tuning case is considered to obtain a particular solution to the equation. In this particular case $\omega \neq \omega_0$ and $\zeta \neq \zeta_0$, meaning there is no resonance between the oscillator and the structure. Given these conditions, utilizing Eq. (2-2) and again only considering lightly damped systems, yielding the assumption $\omega_{0,d} \approx \omega_0$ and $\omega_d \approx \omega$, the following relationship for the FRS value $S_F(\omega_0, \zeta_0)$ can be obtained

$$S_F^2(\omega_0, \zeta_0) = |\ddot{u}_F(t)|_{max}^2 = AF_0^2 \cdot S_A^2(\omega_0, \zeta_0) + AF^2 \cdot S_A^2(\omega, \zeta) \tag{2-6}$$

where $S_A(\omega_0, \zeta_0)$ and $S_A(\omega, \zeta)$ are the corresponding GRS values for the pairs of frequency and damping of the oscillator and the structure, respectively. The parameters AF_0 and AF are amplification factors, which for the non-tuning case can be written as

$$AF_0 = \frac{r^2}{\sqrt{(1-r^2)^2 + 4(\zeta_0^2 + \zeta^2)r^2 - 4\zeta_0\zeta r(1+r^2)}} \qquad (2\text{-}7)$$

$$AF = \frac{1}{\sqrt{(1-r^2)^2 + 4(\zeta_0^2 + \zeta^2)r^2 - 4\zeta_0\zeta r(1+r^2)}}$$

where $r = \omega/\omega_0$.

Since the amplification factors in Eq. (2-7) are derived for the non-tuning case, an extension of the formulation of the amplification factors to also cover perfect tuning and near tuning is required. In the work by Jiang et al. [3] [4], this was achieved by first qualitatively comparing the shape of the amplification factors with the shapes of the dynamic magnification factors (DMF) for a SDOF oscillator subjected to harmonic loading and harmonic base excitation. From the comparison, it was concluded that the shape of AF_0 is similar to the DMF of a SDOF oscillator subjected to harmonic loading whereas AF is similar to the DMF for harmonic base excitation. Based on these findings, Jiang et al. proposed that a generalized form of AF_0 and AF, covering both non-tuning and tuning cases, can be defined as

$$AF_0 = \frac{r^2}{\sqrt{(1-r^2)^2 + \left(2\zeta_{0,e}r\right)^2}} \qquad (2\text{-}8)$$

$$AF = \frac{1}{\sqrt{(1-r^2)^2 + (2\zeta_e r)^2}}$$

where $\zeta_{0,e}$ and ζ_e denote equivalent damping coefficients for the amplification factors of the oscillator and the structure, respectively.

For non-tuning cases, the equivalent damping coefficients are not necessary to determine since the amplification factors are directly given by the relationships in Eq. (2-7). However, for tuning cases, the equivalent damping coefficients must be quantified. Hence, to obtain a general formulation of the method, Jiang et al. derived relationships for $\zeta_{0,e}$ and ζ_e by investigating an arbitrary perfect tuning case, i.e. when $\omega_0 = \omega$ and $\zeta_0 = \zeta$. Starting from the definition of $C(t) = h_0(t) * h(t)$ in Eq. (2-3), the derivation yields the following expression for the FRS value $S_f(\omega, \zeta)$ in the perfect tuning case

$$S_f(\omega,\zeta) = \frac{1}{2}\Big|-\omega^2 t e^{-\zeta\omega t}\cos(\omega t) * \ddot{u}_g(t) + \omega e^{-\zeta\omega t}\sin(\omega t) * \ddot{u}_g(t)\Big|_{max} = S_A^t(\omega,\zeta) \qquad (2\text{-}9)$$

where $S_A^t(\omega, \zeta)$ denotes the spectral response in a tuning-type Response Spectrum called tRS by Jiang et al. [3] [4] [5]. The concept of evaluating a tRS is similar to that of a GRS. In a GRS, the maximum response of a SDOF oscillator mounted directly on the ground and subjected to the ground motion $\ddot{u}_g(t)$ is evaluated. In a tRS, the maximum response is instead evaluated for a SDOF oscillator mounted on top of a SDOF structure that is mounted on the ground and subjected to the ground motion

$\ddot{u}_g(t)$. Note that the SDOF structure and oscillator are defined with the same frequency and damping (perfect tuning) and uncoupled in the evaluation. The latter condition means that the response of the SDOF structure is used as input excitation on the SDOF oscillator without considering any interactions between the two SDOFs. From the response obtained in the SDOF oscillator, the maximum response is then determined to obtain the spectral response of the tRS for the considered frequency and damping, which can be directly obtained by evaluating the expression in Eq. (2-9). The conceptual procedure of determining the spectral response of a tRS is illustrated in Figure 2-1, and also compared to the corresponding procedure for a GRS.

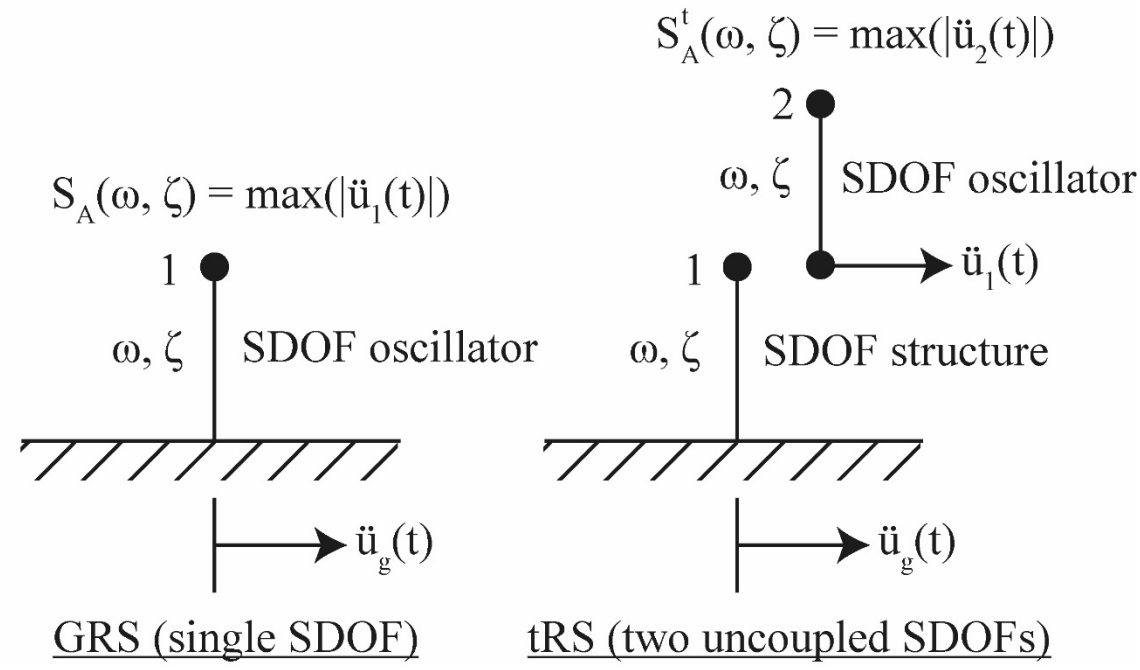

Figure 2-1 Schematic illustration of the procedures to determine a GRS (left side) and a tRS (right side).

The FRS value in the perfect tuning case according to Eq. (2-9) can be expressed on the same form as the FRS value given in Eq. (2-6). In the perfect tuning case when $\omega_0 = \omega$ and $\zeta_0 = \zeta$, the following must hold: $r = 1$, $S_A(\omega_0, \zeta_0) = S_A(\omega, \zeta)$ and $AF_0 = AF$. Given these conditions, Eq. (2-6) can be rewritten as

$$S_f(\omega, \zeta) = \sqrt{2} \cdot AF \cdot S_A(\omega, \zeta) = S_A^t(\omega, \zeta) \tag{2-10}$$

which also leads to the following relationship for the perfect tuning case

$$AF = AF_0 = \frac{1}{\sqrt{2}} \cdot \frac{S_A^t(\omega, \zeta)}{S_A(\omega, \zeta)}. \tag{2-11}$$

In addition, the relationships of the amplification factors in Eq. (2-8) can be rewritten as

$$AF_0 = \frac{1}{2\zeta_{0,e}} \qquad (2\text{-}12)$$

$$AF = \frac{1}{2\zeta_e}.$$

Since $AF_0 = AF$, combining Eqs. (2-11) and (2-12) yields the following relationship for the equivalent damping coefficients in the perfect tuning case

$$\zeta_e = \zeta_{0,e} = \frac{1}{\sqrt{2}} \cdot \frac{S_A(\omega,\zeta)}{S_A^t(\omega,\zeta)}. \qquad (2\text{-}13)$$

According to the work by Jiang et al [4], one cannot obtain an exact expression for the near-tuning case. Instead, they suggest that the following approximations of the equivalent damping coefficients may be used for all possible cases, i.e. in non-tuning, tuning and near-tuning cases

$$\zeta_{0,e} = \frac{\sqrt{2}\zeta_0}{\zeta_0 + \zeta} \cdot \frac{S_A(\omega_0,\zeta_0)}{S_A^t(\omega_0,\zeta_0)} \qquad (2\text{-}14)$$

$$\zeta_e = \frac{\sqrt{2}\zeta}{\zeta_0 + \zeta} \cdot \frac{S_A(\omega,\zeta)}{S_A^t(\omega,\zeta)}.$$

It should be noted that the expressions in Eq. (2-14) reduces to Eq. (2-13) in the perfect tuning case when $\zeta_0 = \zeta$.

According to Eq. (2-9), in the perfect tuning case, the FRS value is equal to the spectral response value of the tRS. However, because of the time variable in the first convolution term, it is hard to find an analytical solution to Eq. (2-9) expressed in terms of the GRS. Hence, in the DSSM developed by Jiang et al. [3] [4], they instead suggest that the tRS is explicitly evaluated from either real earthquake records or synthesized time signals based on the design GRS at the site. To overcome this limitation of their proposed method, they developed a set of statistical relationships to obtain the tRS directly from a GRS, which are presented in reference [5]. The relationships were obtained from regression analysis of evaluated tRS based on a large number of earthquake records from north America utilizing the expression in Eq. (2-9). However, it should be noted that these statistical relationships are not applicable for the Swedish earthquake. In the examples of this study, presented in section 3, the tRS was instead directly evaluated from synthesized time signals obtained from the Swedish GRS at hard rock sites using Eq. (2-9).

2.2.1 SDOF oscillator mounted on MDOF structure

The relationships outlined above are applicable for a SDOF oscillator mounted on a SDOF structure. However, most real engineering structures consist of multiple degrees of freedom (MDOF). Hence, in the work by Jiang et al [3] [4], the formulation of the method was extended to cover the more generic case of a SDOF oscillator mounted on a MDOF structure. Using the principles of modal

analysis/mode superposition to derive an expression for the response of the oscillator, and combining the result with Eq. (2-6), the following relationship was obtained for a SDOF oscillator with circular frequency ω_0 and damping ζ_0

$$R^i_{n,j;k} = \varphi_{n,j;k}\Gamma^i_k\sqrt{AF^2_{0,k}\cdot\left[S^i_A(\omega_0,\zeta_0)\right]^2 + AF^2_k\cdot\left[S^i_A(\omega_k,\zeta_k)\right]^2}. \tag{2-15}$$

In the equation, $R^i_{n,j;k}$ denotes the response contribution of the k:th mode to the maximum absolute acceleration of the oscillator, $S^i_{n,j}$, in direction j, under earthquake excitation in direction i and mounted at node n in the MDOF structure. In the context of a FE model of a structure, the direction j denotes the direction/rotation of the currently considered DOF in the FE model. The parameters $\varphi_{n,j;k}$ and Γ^i_k denote the mode shape in mode k (i.e. the normalized displacement of node n in direction j) and the participation factor in earthquake direction i for mode k, respectively. The spectral acceleration $S^i_A(\omega_0,\zeta_0)$ is the GRS value in earthquake direction i using the frequency and damping of the oscillator and $S^i_A(\omega_k,\zeta_k)$ is the corresponding value given by the frequency (ω_k) and damping (ζ_k) of the k:th mode of the structure. The amplification factors are given by the following relationships, which stems from Eq. (2-8) above

$$AF_{0,k} = \frac{r_k^2}{\sqrt{(1-r_k^2)^2 + \left(2\zeta_{0,k,e}r_k\right)^2}} \tag{2-16}$$

$$AF_k = \frac{1}{\sqrt{(1-r_k^2)^2 + \left(2\zeta_{k,e}r_k\right)^2}}$$

where $r_k = \omega_k/\omega_0$. The equivalent damping coefficients are defined on the same form as in Eq. (2-14), but adjusted to consider the frequency and damping of the k:th mode

$$\zeta_{0,k,e} = \frac{\sqrt{2}\zeta_0}{\zeta_0+\zeta_k}\cdot\frac{S_A(\omega_0,\zeta_0)}{S^t_A(\omega_0,\zeta_0)} \tag{2-17}$$

$$\zeta_{k,e} = \frac{\sqrt{2}\zeta_k}{\zeta_0+\zeta_k}\cdot\frac{S_A(\omega_k,\zeta_k)}{S^t_A(\omega_k,\zeta_k)}.$$

To obtain the total maximum absolute acceleration of the oscillator in direction i, $S^i_{n,j}$, the response contributions from each mode, $R^i_{n,j;k}$, must be combined using a suitable combination rule. In normal response spectrum analysis of structures, the complete quadratic combination (CQC) rule is often used for modal combination, and is also recommended in ASCE 4-16 [2]. For the modal combination of the response in the oscillator, Jiang et al. [3] [4] developed a similar complete quadratic rule called FRS-CQC. This new modal combination rule was developed based on random vibration theory, and does not only take into account the correlation between the modal response of the structure but also the correlation between the response of the oscillator and the structural modes. The derived relationship is

quite long and is not presented in this report, but can be found in [3] or [4]. The resulting correlation coefficient $\rho_{k\kappa}$, or mode interaction coefficient, depends on the frequency and damping of the oscillator and the structure. In the regular CQC rule, the correlation coefficient is only a function of the frequency and damping of the structure. Using the correlation coefficient, the maximum absolute acceleration of the oscillator in direction j, caused by earthquake excitation in direction i, is obtained by combining the contributions from the k modes according to

$$S_{n,j}^{i}(\omega_0, \zeta_0) = \sqrt{\sum_{k=0}^{N}\sum_{\kappa=0}^{N} \rho_{k\kappa}(\zeta_0, r_k, \zeta_k, r_\kappa, \zeta_\kappa) R_k^i R_\kappa^i} \tag{2-18}$$

where N denotes the number of eigenmodes, k and κ denote mode numbers, $r_k = \omega_k/\omega_0$ and $r_\kappa = \omega_\kappa/\omega_0$. The variation of the correlation coefficient $\rho_{k\kappa}$ for values of r_k and r_κ in the range 0 to 2.5, and using the damping values $\zeta_0 = \zeta_k = \zeta_\kappa = 5$ %, is illustrated in Figure 2-2.

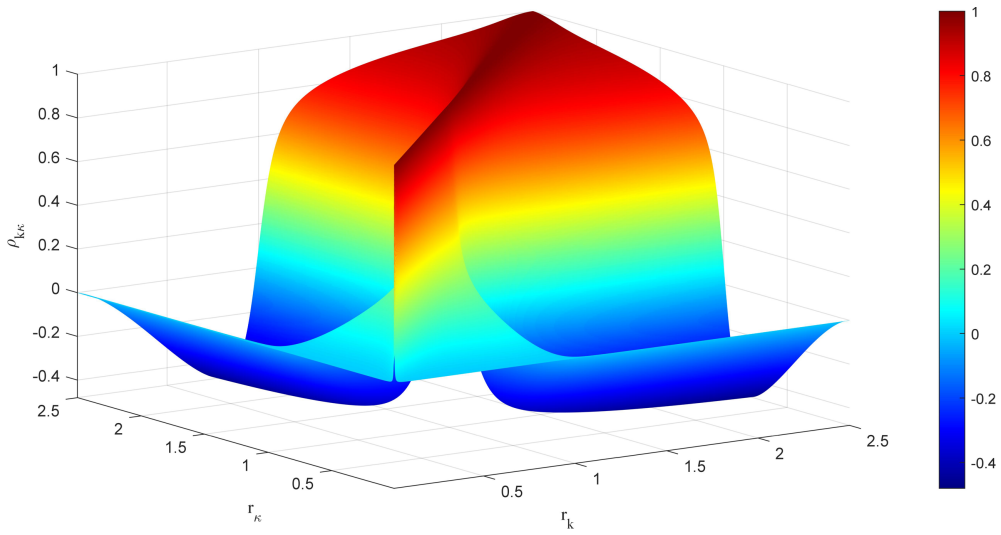

Figure 2-2 Variation of the correlation coefficient for values of r_k and r_κ in the range 0 to 2.5 and damping values $\zeta_0 = \zeta_k = \zeta_\kappa = 5$ %.

The total FRS of an oscillator mounted on node n in direction j, $S_{n,j}(\omega_0, \zeta_0)$, under tri-axial earthquake excitation is then obtained using the SRSS (Square Root of Sum of the Squares) combination rule

$$S_{n,j}(\omega_0, \zeta_0) = \sqrt{\sum_{i=1}^{3} \left[S_{n,j}^{i}(\omega_0, \zeta_0)\right]^2}. \tag{2-19}$$

It should be noted that the SRSS rule is recommended in ASCE 4-16 [2] for spatial combination of the components when performing modal analysis.

2.2.2 Summary of Jiang's method

The generic algorithm to evaluate a FRS using Jiang's proposed DSSM is presented in Figure 2-3. It also includes references to the relevant equations presented in the previous section.

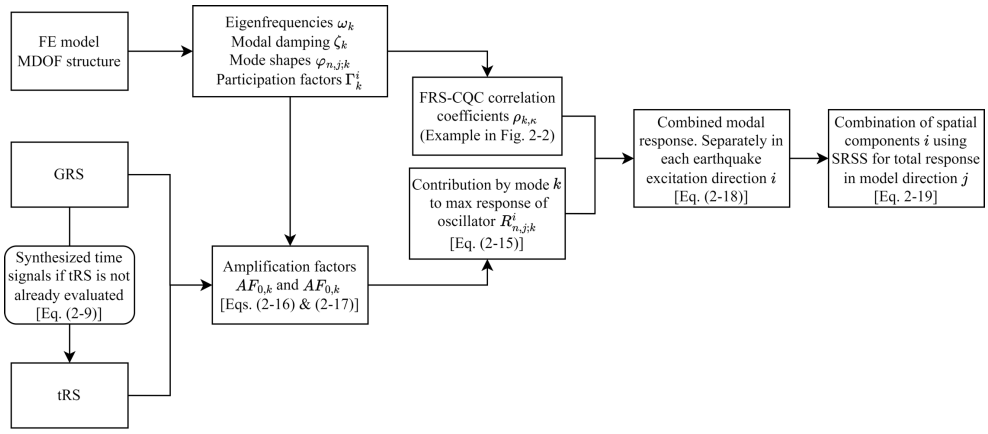

Figure 2-3 Summary of algorithm for Jiang's proposed DSSM together with references to the relevant equations in section 2.2.1.

The algorithm presented above can be implemented in any computer code of choice. In this study, the method was implemented in MATLAB. The complete developed set of MATLAB scripts for evaluation of FRS using Jiang's method is attached to this report in a zip-archive. The archive also includes all relevant input data for evaluation of the FRS in the examples presented in sections 3 and 4. A summary and short description of the files included in the zip-archive can be found in Appendix A:.

2.3 THE PSD METHOD

An alternative method, based on spectrum-compatible random processes, was tried out for comparison in the evaluation of Jiang's method. It has been identified as promising, although it is difficult to find other research on earthquake analysis using this method. In this report, the ambition is limited to sharing the outline of the method, with the ambition to continue the development and verification of the method in future work.

This alternative PSD method can be compared to the current praxis for calculation of FRS using a set of spectrum-compatible time series, especially when the time-series are synthesised through realisations of a random process. The difference lies in the use of the underlying process and its statistical properties, instead of creating many realisation examples of the process. Hence, this alternative method avoids the problem with natural random variation in FRS output from a single process realisation to another. In addition, it avoids the necessity of running several computationally expensive time history analyses, and instead relies on the structure's modal properties, i.e. similarly to other DSSMs proposed in the literature.

Linear system dynamics is assumed in our effort to find the FRS in a building. Given this fundamental assumption, any stationary Gaussian (normal probability distribution) random vibration (ground) excitation will result in a stationary Gaussian random response vibration for each position and direction of the linear primary structure (building). In addition, if the stationary Gaussian random vibration is zero-mean, as earthquake motions are, it is completely described by a Power Spectral Density (PSD), which is the Fourier transform pair to the auto-correlation function of the random vibration. Hence, the PSD is a description of the random vibration excitation that is as compact as a response spectrum. The shape of the PSD is determined by the random vibration energy distribution over the frequency range, and it determines the shape of the response spectrum of the same random vibration. However, the response spectrum amplitudes of a random vibration are not distinct since the response spectrum of a random vibration is also depending on the vibration duration. There is no limit in the extreme value of the random vibration with normal distribution, only a probability of exceedance or a calculated expectation of a maximum value. The longer you observe the Gaussian vibration, the higher maximum value is expected.

A response spectrum is calculated using a set of linear SDOF systems, like the system depicted in Figure 2-4. The steady-state acceleration response PSD of a SDOF system's mass to a stationary random base excitation, with a one-sided PSD, $G_{XX}(f)$, is calculated as the product of the squared transfer function magnitude and the excitation PSD,

$$G_{YY}(f) = |H_{XY}|^2(f) G_{XX}(f). \quad (2\text{-}20)$$

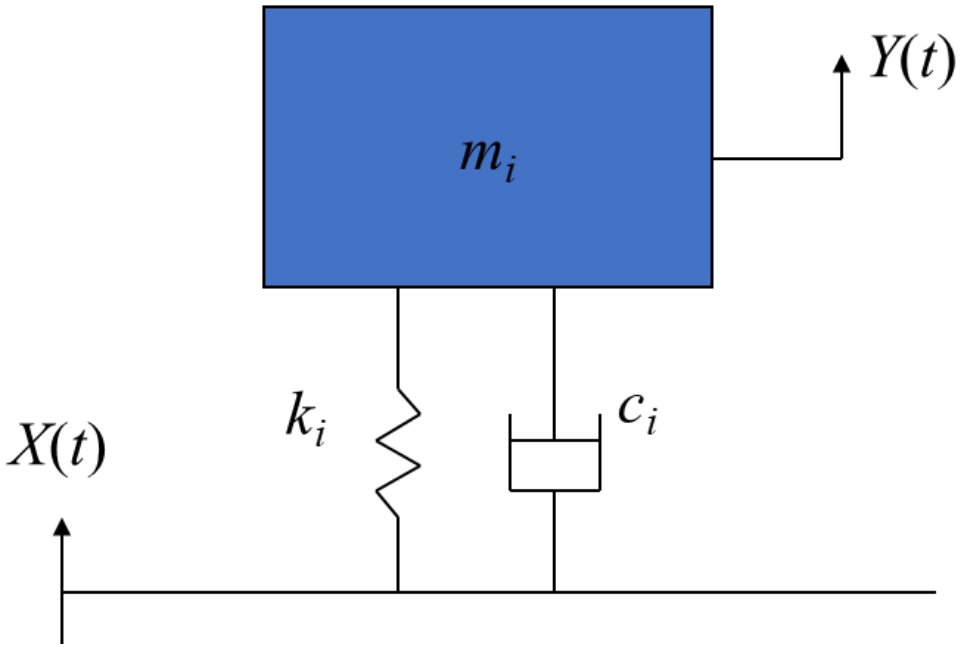

Figure 2-4 Sketch of SDOF-system *i* used in response spectrum calculations. Transfer function between random acceleration input *X(t)* and response acceleration *Y(t)* is derived from the mass, stiffness and damping.

The mean square of the response is derived from its PSD as

$$\sigma_Y^2 = \int_0^\infty G_{YY}(f)df. \tag{2-21}$$

Lalanne [6] [7], see also [34] for more details, presents an approximative expression for the expected maximum value of the response acceleration during observation duration T as

$$E\left[\max\left(Y|_{t=[0,T]}\right)\right] = \sigma_Y\sqrt{2ln(n_0^+T)}\,, \tag{2-22}$$

where n_0^+ is the expected number of zero-level-crossings with a positive slope per unit of time. Just as σ_Y, n_0^+ is only depending on the PSD $G_{YY}(f)$ through its spectral moments as

$$n_0^+ = \sqrt{m_2/m_0}\,, \tag{2-23}$$

where the spectral moments are defined as

$$m_k = \int_0^\infty f^k G_{YY}(f)df\,. \tag{2-24}$$

Hence, the expected maximum value of a zero mean stationary Gaussian random vibration during a time period of length T can be calculated as long as you know its PSD. Remember also that the PSD describes this random vibration completely.

The expected maximum response acceleration of a SDOF system's mass, when subjected to stationary random ground vibration, becomes the response spectrum amplitude for the frequency corresponding to the natural frequency of the particular SDOF system. Then the calculation procedure is repeated for all SDOF systems with different natural frequencies until the complete response spectrum is obtained.

This repetitive calculation procedure is difficult to inverse, so finding the PSD of a response spectrum-equivalent stationary random vibration is not trivial. The authors do it by an iterative procedure with repetitive adjustments of the PSD, until the forward calculation procedure ends up with a close enough response spectrum.

Having found the response spectrum-equivalent PSD, the next step concerns the analysis of the primary building structure. Mass and stiffness matrices of the linear FE model are used together with the damping of the structure to derive the transfer functions from each ground excitation direction to the output (floor) accelerations, where FRS need to be determined. The transfer functions are then used to calculate the floor response PSDs, through the simple multiplication in the frequency domain. In the final step, each FRS is calculated from the floor response PSD using the same repetitive calculation procedure with expected maximum values as described above.

Finding the transfer functions is just as effortless as doing the response calculation by frequency domain multiplication. Hence, there is a substantial computation time advantage with the PSD method compared to the time series method of current praxis in Sweden and Finland. Another advantage is that you get one result, corresponding to the response spectrum expectation in a probabilistic sense, without having to do lots of sampling and averaging.

It is not clear to the authors why earthquake analysis research using PSD-equivalent response spectrum is scarce in the literature. A possible reason may have to do with the assumption about stationarity, which is necessary to make the PSD a complete description of the random vibration. The PSD method is assuming a zero-mean stationary Gaussian ground motion, but it is clear that, although the random behaviour of true earthquake motion is not questioned, the assumption about stationarity is not fully correct. In addition, the short time duration of the strong part of an earthquake makes it debateable to ignore the transient solution of the vibration response and only use the steady state solution resulting from the transfer function multiplication in the frequency domain.

Despite the simplifying assumptions, the PSD method was implemented and its performance compared to Jiang's method and the time history analysis method. The choice is motivated by the simplicity of the calculations and a belief that the introduced assumptions do not significantly affect the result, i.e. the FRS.

3 Evaluation of DSSMs – Description of examples

To assess the performance of the two DSSMs described in sections 2.2 and 2.3, FRS are developed in a number of selected points in two example structures. As reference solutions, FRS are also developed from THA. The latter FRS are based on five sets of acceleration time series, which then are averaged to obtain a single FRS in each direction at the selected points, i.e. in accordance with ASCE 4-16 [2]. The FE-models of the example structures are developed in the commercial finite element code Abaqus [35], version 2022.HF4.

In this section, the two example structures and the used input data are described, whereas the results are presented and discussed in section 4. The first example aims to resemble a typical Swedish BWR containment structure, whereas the second example resembles a generic service building at a nuclear facility with more closely space modes.

3.1 EXAMPLE STRUCTURES

3.1.1 Example 1 – Simplified containment structure

The first example aims to resemble a typical Swedish BWR containment structure including the pool structure located on top of the cylindrical containment wall. Both the containment and the pool are assumed to consist of reinforce concrete. The used simplified geometry is based on a model from a previous study by Rydell et al. [36].

Geometry

The simplified containment structure consists of a cylindrical containment wall together with a pool situated on its upper surface. It should be noted that no water is considered in the pool. The containment wall is modelled with beam elements having a pipe-shaped cross section, whereas the pool structure is modelled with shell elements. The modelled geometries of these structural parts are illustrated in Figure 3-1.

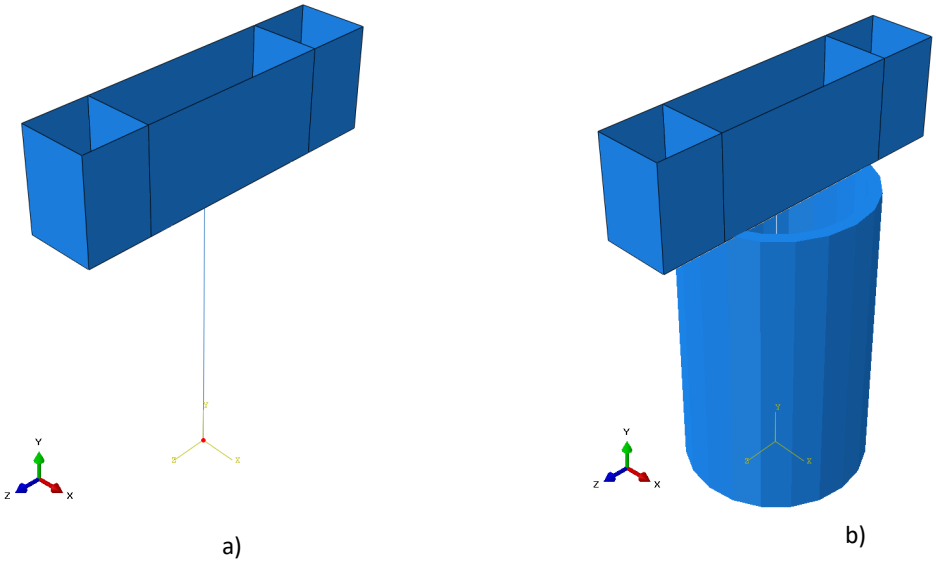

Figure 3-1. a) Modelled geometry of the simplified containment structure. b) Rendering of the cross-sectional shape of the beam element resembling the containment wall.

The dimensions of the containment and the pool structure in the analysis are summarised below:

- Dimensions of the containment:
  - Height: 40 m
  - Outer radius: 12.1 m
  - Wall Thickness: 1.6 m
- Dimensions of the pool:
  - Thickness of outer walls: 1.1 m
  - Thickness of pool bottom: 1.1 m
  - Thickness of inner walls: 1 m
  - Wall height: 13 m
  - Pool length: 42 m
  - Pool width: 10 m
  - Distance to inner walls from short side of pool: 8.5 m

Boundary conditions and couplings

Boundary conditions were only applied on the bottom node of the containment in the model, see the red dot in Figure 3-1 a). At this node, all translational and rotational degrees of freedom were restrained using a Dirichlet condition in the eigenfrequency analysis. Regarding the applied earthquake excitation, see section 3.3. In addition to the boundary conditions, a coupling constraint was defined between the top node of the containment and a part of the bottom surface of the pool, see Figure 3-2.

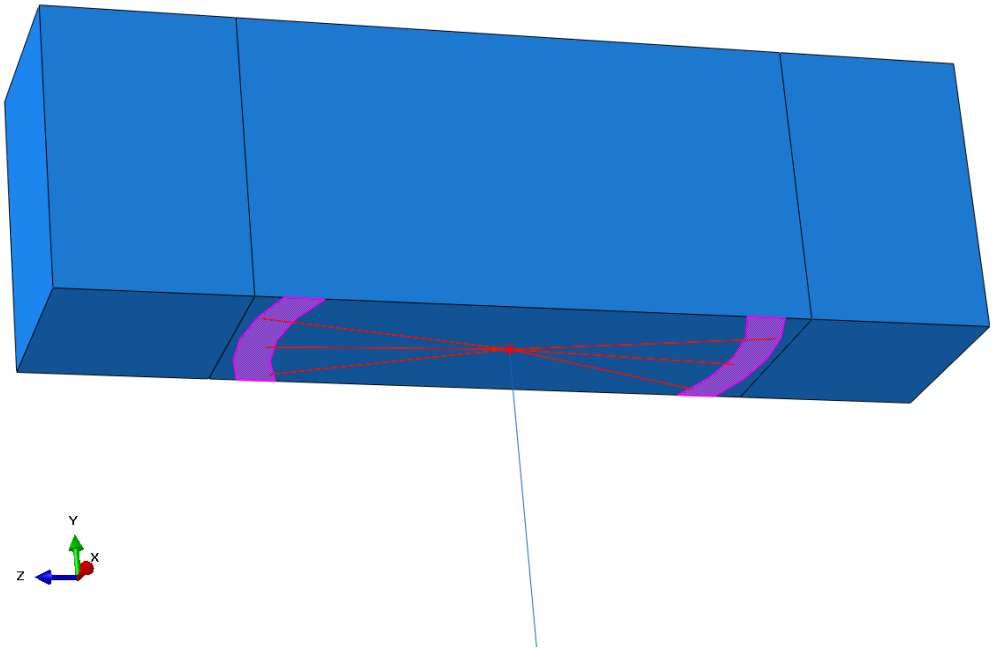

Figure 3-2 Defined coupling constraint between the top node of the containment (red dot) and part of the bottom surface of the pool (purple surface).

All degrees of freedom were constrained in the defined coupling. Note that the purple surface in Figure 3-2, over which the coupling was defined, corresponds to the contact surface between the cylindrical wall and the pool.

Mesh

The cylindrical containment was meshed with linear beam elements (denoted B31 in Abaqus), whereas the pool was meshed using linear shell elements with reduced integration (denoted S4R in Abaqus). All elements in the model have an average element length of approximately 0.4 m. The mesh of the pool is shown in Figure 3-3.

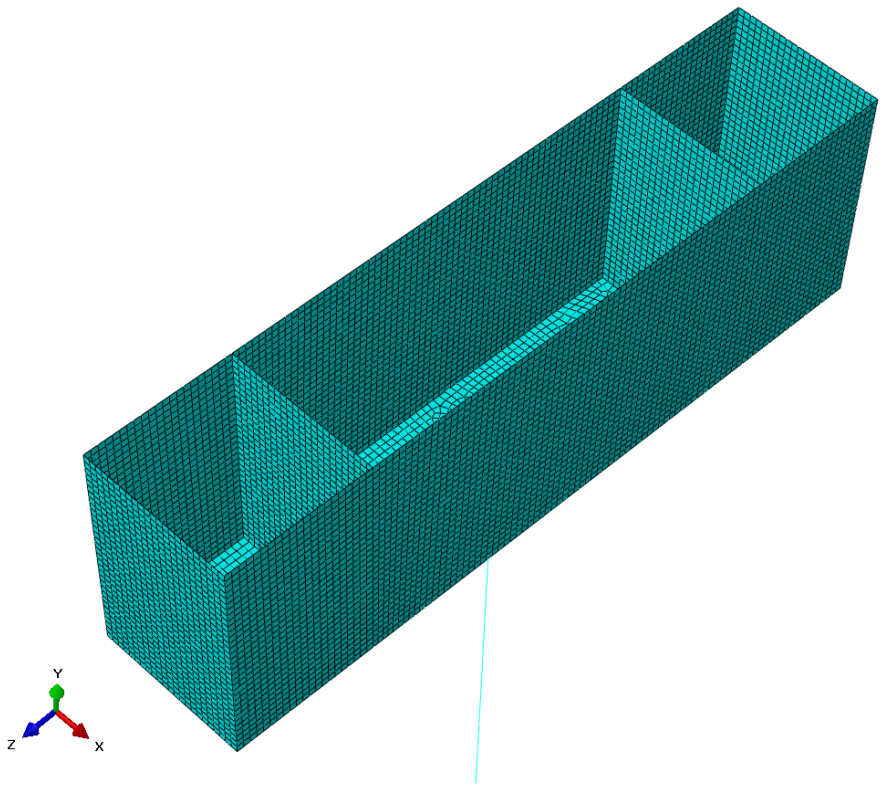

Figure 3-3 Mesh of the pool.

The total number of nodes, elements and degrees of freedom in the model are 12927, 12683 and 76362, respectively.

3.1.2 Example 2 – Generic service building

The second example aims to resemble the structural system of a generic service building at a nuclear facility. The structure is stiffer in its horizontal directions compared to the simplified containment building in Example 1, and also has more closely spaced modes. All structural elements of the building are assumed to consist of reinforced concrete.

Geometry

The geometry of the analysed service building is shown in Figure 3-4.

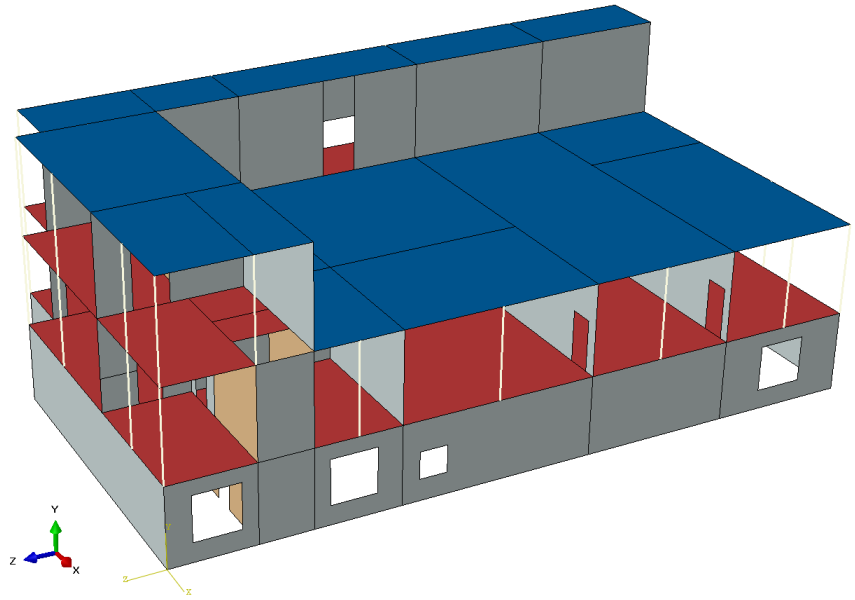

a)

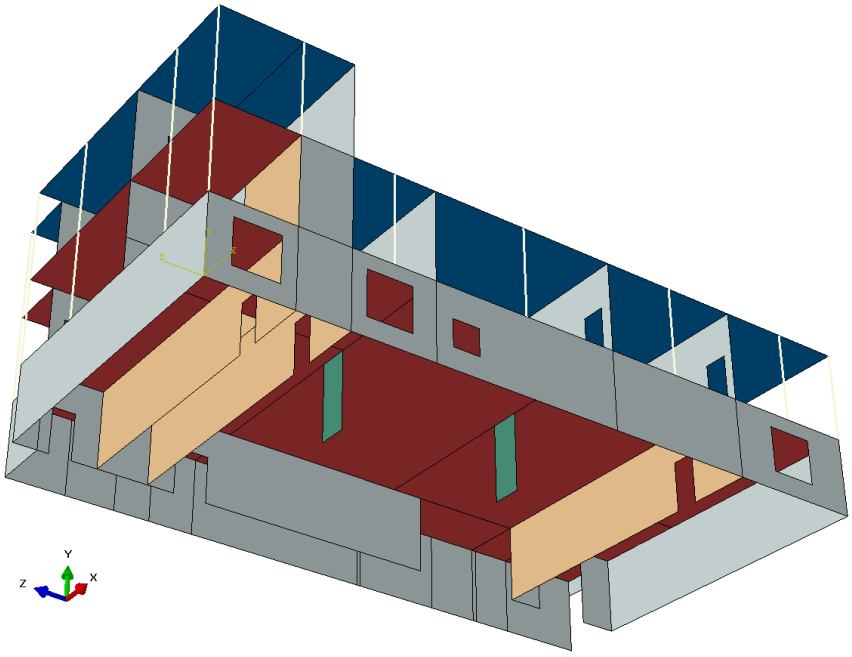

b)

Figure 3-4 Modelled geometry of the analysed service building in Example 2.

The service building is 17.2 m wide, 30.15 m long and has a height of 11.8 m at its highest point above ground level. The coloured shell elements in Figure 3-4 have been defined with the following thicknesses:

- Blue (roof): 0.2 m
- Red (floor): 0.3 m
- Gray (walls): 0.25 m
- Orange (walls): 0.3 m

- Green (walls/columns): 0.3 m

As can be seen in the figure, there are also a number of columns along the periphery of the building on the second and third floor. All these columns have been defined with a 300x300 mm rectangular cross section.

Boundary conditions

All translational and rotational degrees of freedom were restrained at the bottom of all walls in the eigenfrequency analysis of the building, see Figure 3-5. Regarding the applied earthquake excitation, see section 3.3.

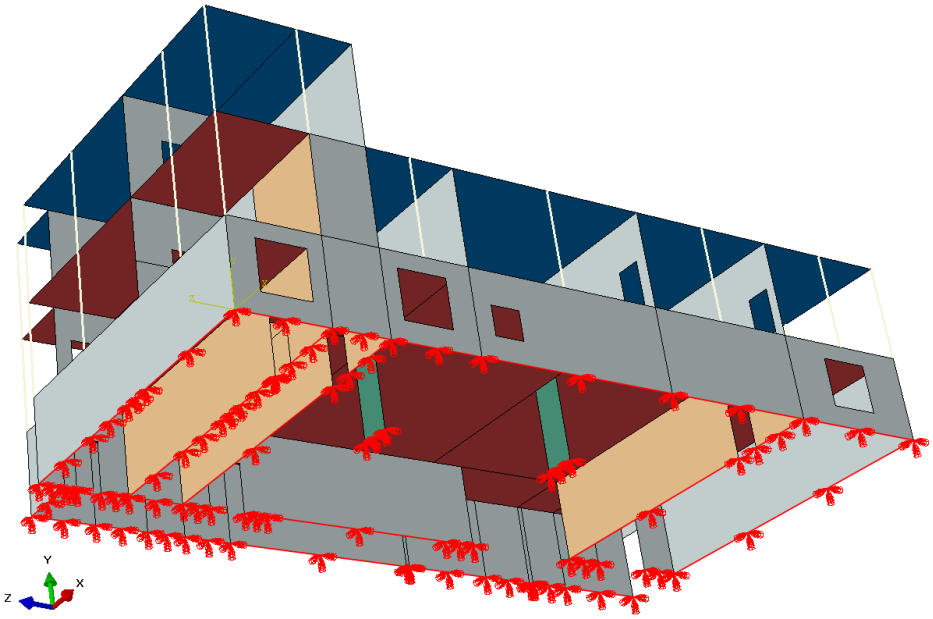

Figure 3-5 Applied boundary conditions in the service building model. All translational and rotational degrees of freedom are restrained on the marked boundaries.

Mesh

The mesh of the service building is shown in Figure 3-6.

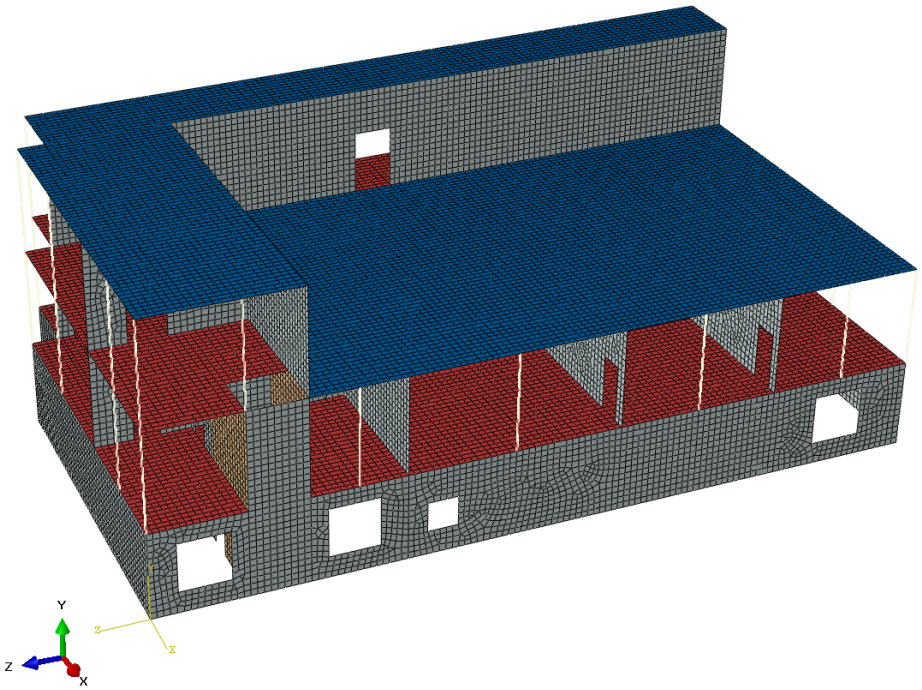

Figure 3-6 Mesh of the service building.

All shells in the model have been meshed using linear shell elements with reduced integration (denoted S4R in Abaqus), whereas the columns are meshed with linear beam elements (denoted B31 in Abaqus). The elements in the model have an average element length of approximately 0.25 m. The total number of nodes, elements and degrees of freedom in the model are 40910, 39842 and 239952, respectively.

3.2 MATERIAL AND DAMPING

All structural members in both examples are assumed to consist of concrete and modelled using a linear elastic material model. The following material properties have been used:

- Density: 2400 kg/m^3
- Elastic modulus: 30 GPa
- Poisson's ratio: 0.2

In both examples, a uniform modal damping with a critical damping fraction equal to 5 % was used for all modes of the structures. The same damping fraction was used for the oscillator when evaluating the FRS from the THA as well as using the two studied DSSMs.

3.3 LOADING

The loading in the two examples consists of the dead weight of the structures as well as the earthquake excitation simultaneously in three orthogonal directions. The former load was applied as body load (volume load) directly in the FE-model prior to the eigenfrequency and/or THA.

In the performed THA, which are utilised as reference solutions for comparison with the DSSMs, the earthquake excitation is applied using acceleration time series. The accelerations are applied simultaneously in each orthogonal main direction. The earthquakes used in the study correspond to the Swedish earthquake at hard rock sites with an annual exceedance probability of 10^{-6}. The used acceleration time series were synthesised and generated to match the Swedish 10^{-6} design GRS with 5 % damping defined in [37]. The suite of synthesized time series were not developed as a part of this study, but instead obtained from the work presented in [38]. It should be noted that all synthesized time series are ASCE 4-98 [1] compliant.

In the performed THA of the structures' response, the acceleration time series were applied on the same boundaries as the boundary conditions in the eigenfrequency analyses, see sections 3.1.1 and Figure 3-5. Five sets of synthesized acceleration time series were used in the analyses, where each set contains two horizontal and one vertical acceleration time series. This results in 15 time series, five in each horizontal direction and five in the vertical direction. All time histories are 10.24 s long and sampled at a time interval of 0.005 s. One horizontal and one vertical acceleration time series used in the analyses are plotted as examples in Figure 3-7 and Figure 3-8.

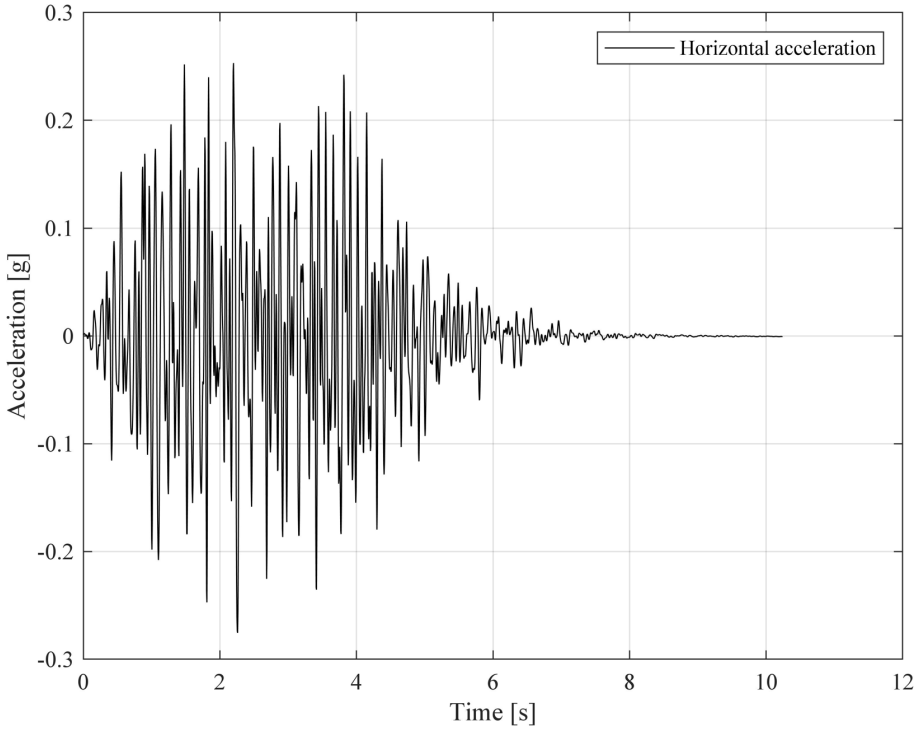

Figure 3-7 Example of horizontal acceleration time series used in the analyses.

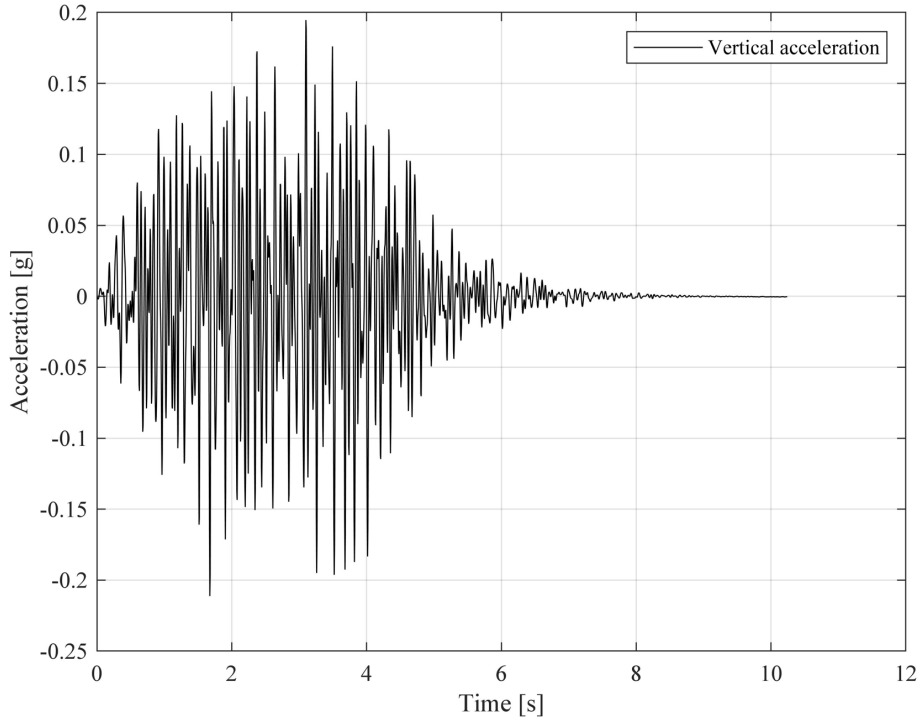

Figure 3-8 Example of vertical acceleration time series used in the analyses.

The horizontal and vertical design GRS with 5 % damping for the Swedish earthquake at hard rock sites with an annual exceedance probability of 10^{-6} are plotted in Figure 3-9 and Figure 3-10, respectively. The 5 % GRS of each

synthesized acceleration time series used as input in the time history analyses are also plotted in the figures. Note that only one horizontal GRS is provided in [37] for the Swedish earthquake, therefore, the same GRS shall be used in both horizontal directions.

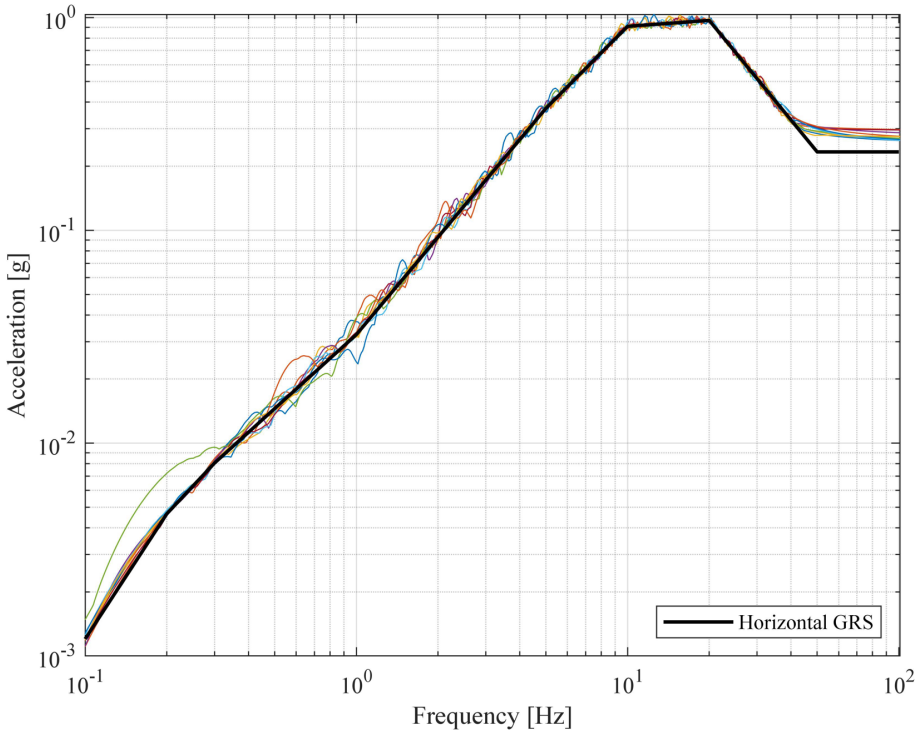

Figure 3-9 Horizontal design GRS with 5 % damping for the Swedish earthquake at hard rock sites with an annual exceedance probability of 10^{-6}, together with the GRS of the ten synthesized acceleration time series used in the THA.

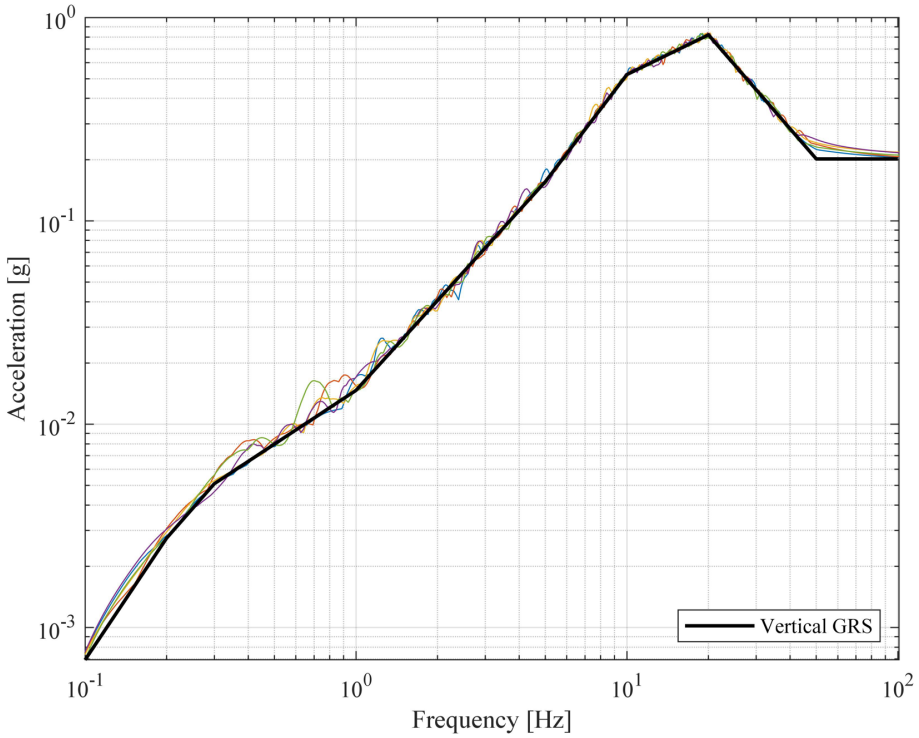

Figure 3-10 Vertical design GRS with 5 % damping for the Swedish earthquake at hard rock sites with an annual exceedance probability of 10^{-6}, together with the GRS of the five synthesized acceleration time series used in the THA.

For development of FRS using Jiang's direct method, the tRS of the earthquake in horizontal and vertical direction are also required as input. As mentioned in section 2.2, the statistical relationship developed in [5] to obtain the tRS directly from the GRS are not applicable for the Swedish earthquake. Instead, the tRS are evaluated directly from the synthesized time series using the relationship expressed in Eq. (2-9). In the vertical direction, the five available time series were used to evaluate the average tRS. For the horizontal direction, all ten time series were used to determine the average tRS, which was then used as input in both horizontal directions when evaluating the FRS using Jiang's DSSM. However, it should be noted that the influence of using two separate tRS in the horizontal directions has also been investigated, see sections 4.1.2 and 4.2.2. The calculated average tRS for the horizontal directions and the vertical direction are plotted in Figure 3-11 and Figure 3-12, respectively. A MATLAB script for calculation of tRS from acceleration time series is included in the zip-archive attached to this report, see Appendix A:.

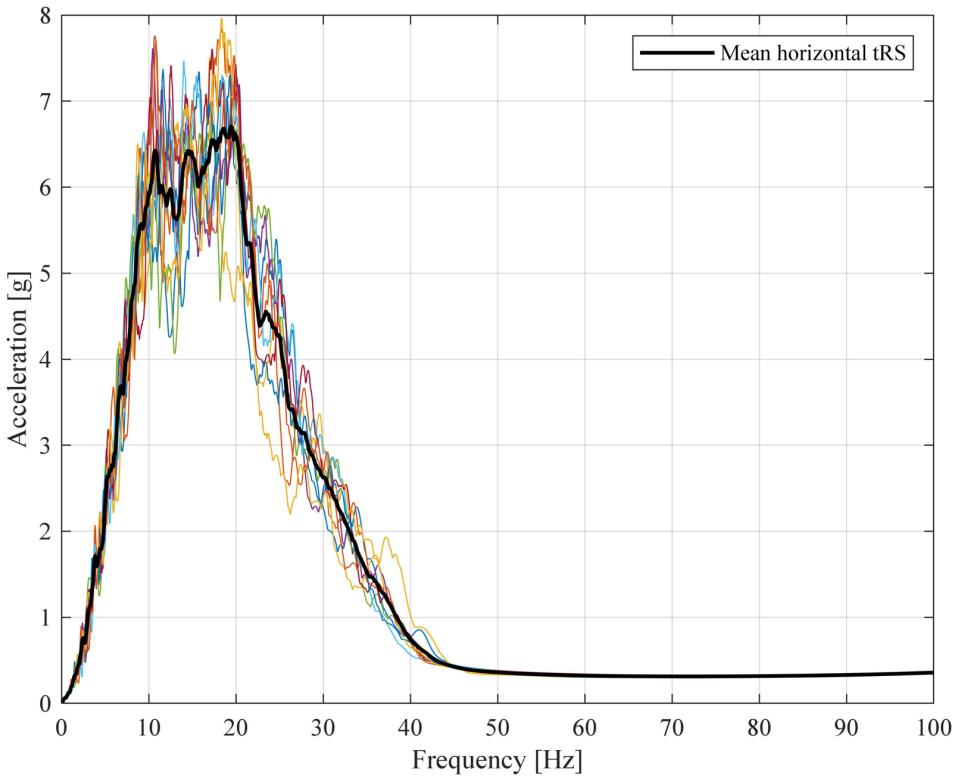

Figure 3-11 Average horizontal tRS evaluated from the ten horizontal acceleration time series. The thin coloured lines show the tRS of each individual time series.

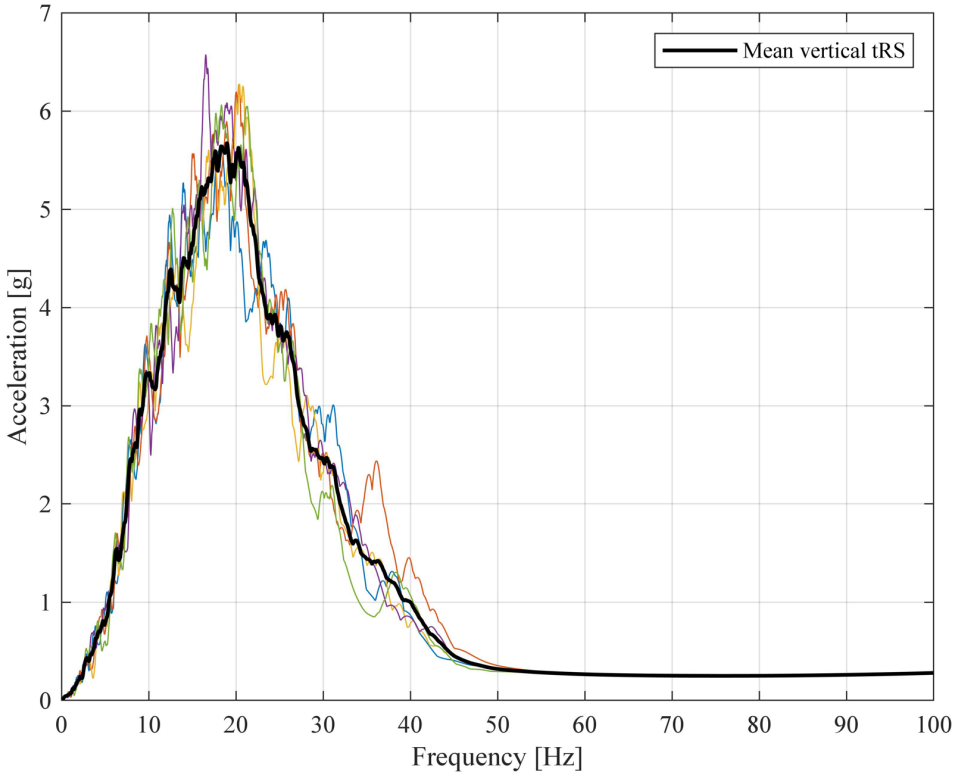

Figure 3-12 Average vertical tRS evaluated from the five vertical acceleration time series. The thin coloured lines show the tRS of each individual time series.

The corresponding equivalent PSD from the Swedish 5 % design GRS for both horizontal and the vertical directions are plotted in Figure 3-13.

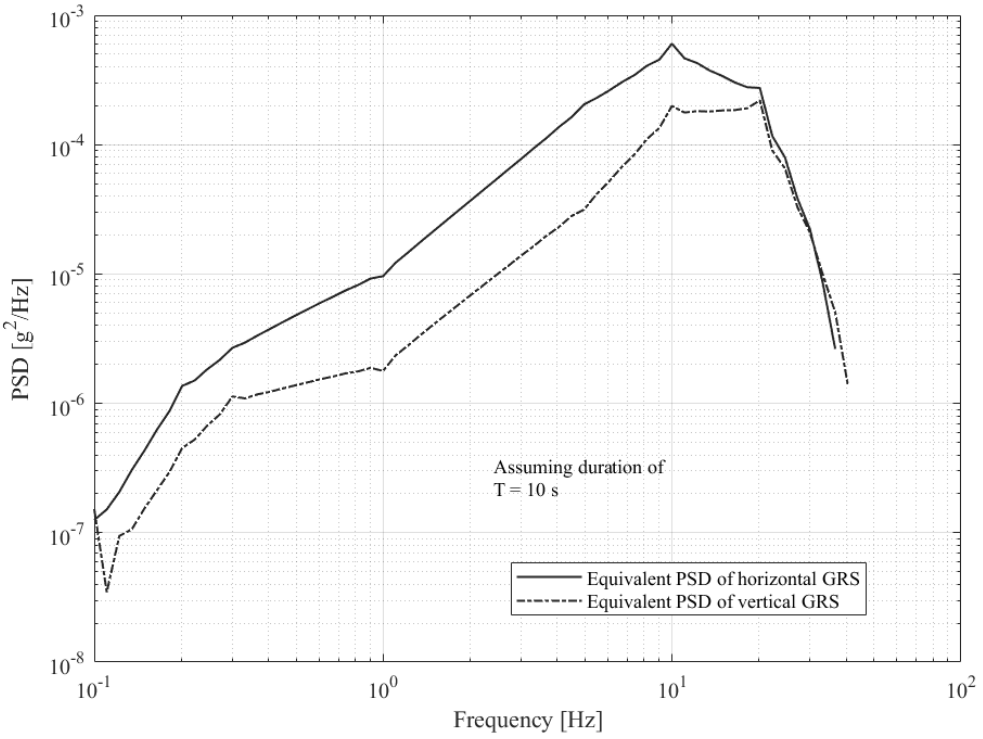

Figure 3-13 Equivalent PSDs evaluated directly from the horizontal and vertical GRS, using formula for expected maximum for a stationary Gaussian vibration, assuming a duration of 10 s.

The GRS that can be obtained from the equivalent PSD in horizontal and vertical directions using Lalanne's formula for expected maximum, Eq. (2-22), are presented in Figure 3-14 and Figure 3-15 to verify that they comply with the 5 % design GRS from [37] used as input. As seen in the figures, the agreement is excellent over all frequencies in the spectra. Note that these plots correspond to the response spectra obtained from the five sets of synthetic acceleration time series presented in Figure 3-9 and Figure 3-10.

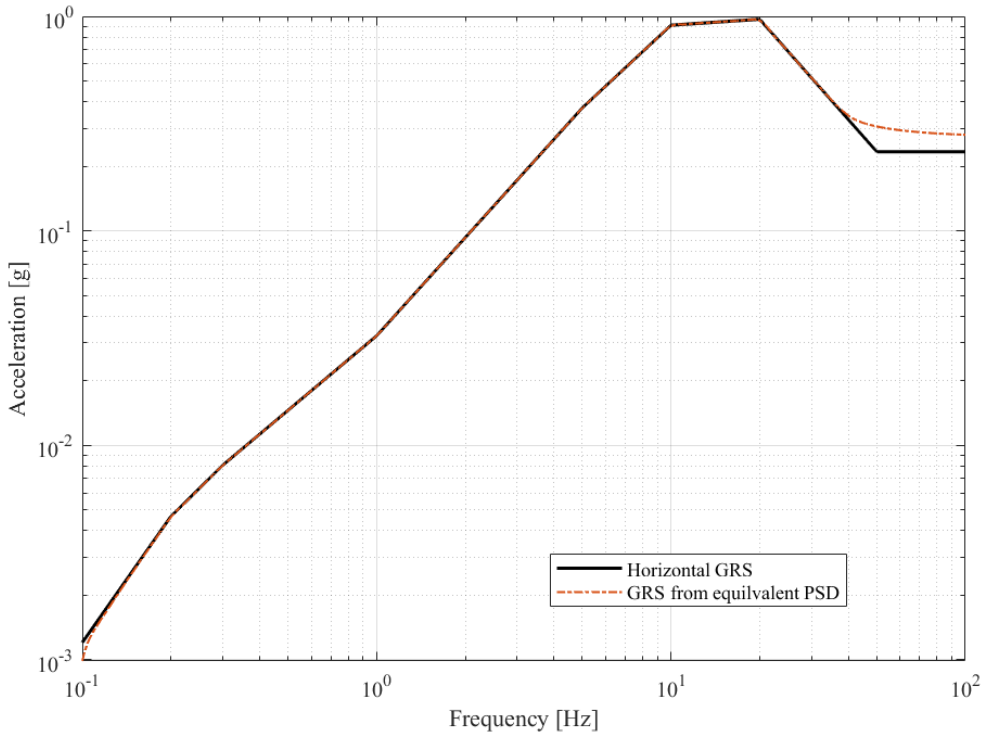

Figure 3-14 Comparison between the horizontal design GRS with 5 % damping from [37] and the GRS acquired from the equivalent PSD in horizontal direction using Lalanne's formula.

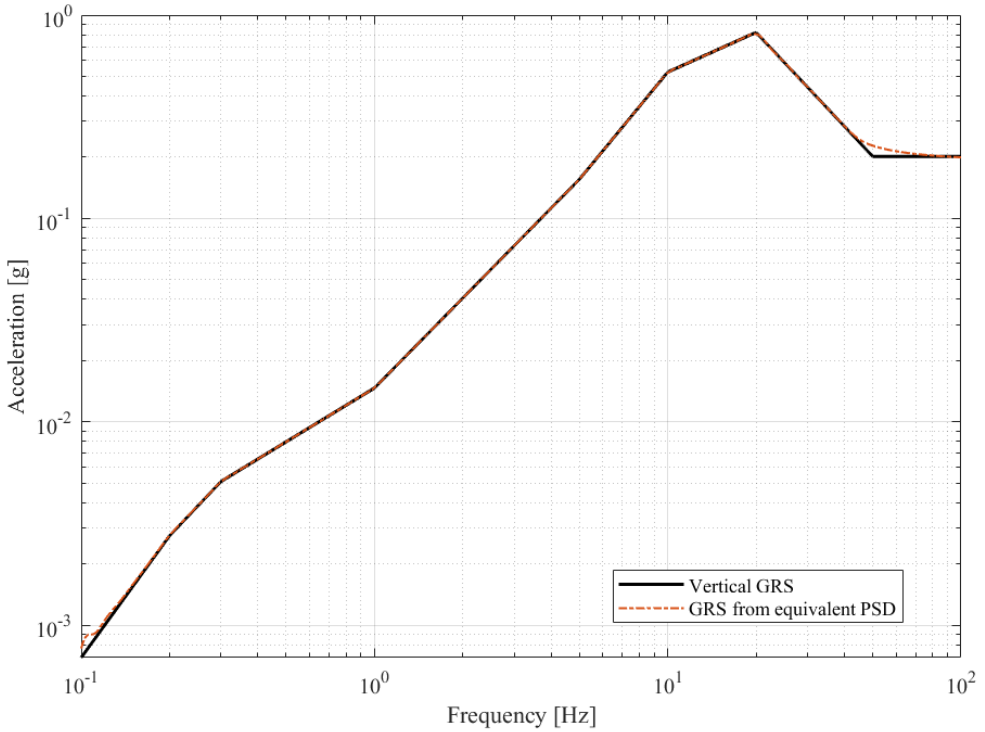

Figure 3-15 Comparison between the vertical 5 % design GRS with 5 % damping from [37] and the GRS acquired from the equivalent PSD in vertical direction using Lalanne's formula.

3.4 FINITIE ELEMENT ANALYSES

According to section 4.2.1 in ASCE 4-16 [2], both direct integration and modal superposition methods can be used to evaluate the linear response-history of structures. Hence, the THA for the five sets of acceleration time series were conducted using a modal superposition method called *Transient modal dynamic analysis* in Abaqus. Furthermore, in the same section of ASCE 4-16, it is stated that the time step in the analysis should not be greater than 0.1 times the shortest period of interest. As mentioned in section 3.3, the acceleration time series were sampled at a time interval of 0.005 s, which corresponds to a Nyquist frequency of 100 Hz. Thus, a time step of $0.1 \cdot 1/100 = 0.001$ s was used in the THA.

In the same section of ASCE 4-16, it is further stated that the number of modes included in the analysis shall be sufficient to ensure that the remaining modes does not increase the response more than 10 %. A similar requirement is also given in section 4.3.3.3.1(3) of Eurocode 8 [39], where it is stated that the sum of the effective modal masses taken into account in the analysis should amount to at least 90 % of the total mass of the structure. In this study, all modes up to 100 Hz have been included in both the transient modal analyses and the eigenfrequency analyses used for input to the two investigated DSSMs. Plots of the effective mass in each direction and further comments related to the above mentioned requirements are given in the result sections 4.1 and 4.2.

All transient modal dynamic analyses were performed in the following steps:

1. Static step: Application of dead weight
2. Eigenfrequency step: Base state of the structure from step 1. Calculation of all modes up to 100 Hz.
3. Transient modal dynamic analysis

At a number of selected nodes in the structure, FRS were calculated from the acceleration response-history at those nodes for each analysed set of acceleration time series. The five obtained FRS in each selected evaluation node and direction were then averaged.

The eigenfrequency analyses performed to obtain the required input data for the investigated DSSMs were performed in the following steps:

1. Static step: Application of dead weight
2. Eigenfrequency step: Base state of the structure from step 1. Calculation of all modes up to 100 Hz.

From the results, the eigenfrequencies and corresponding participation factors were obtained. In addition, the mode shapes (modal nodal displacements) were extracted in each selected evaluation node. No modal damping values were extracted since the same modal damping coefficient was used for all modes in the development of the FRS, see section 3.2.

4 Evaluation of DSSMs – Results and discussion

4.1 EXAMPLE 1 – SIMPLIFIED CONTAINMENT STRUCTURE

4.1.1 Eigenfrequencies

The obtained eigenfrequencies of the structure up to 100 Hz are plotted in Figure 4-1 together with the cumulative effective mass in each main direction of the model. Note that the effective mass is expressed as the fraction of the total mass ($1.60 \cdot 10^7$ kg) of the model. The total number of modes is 114.

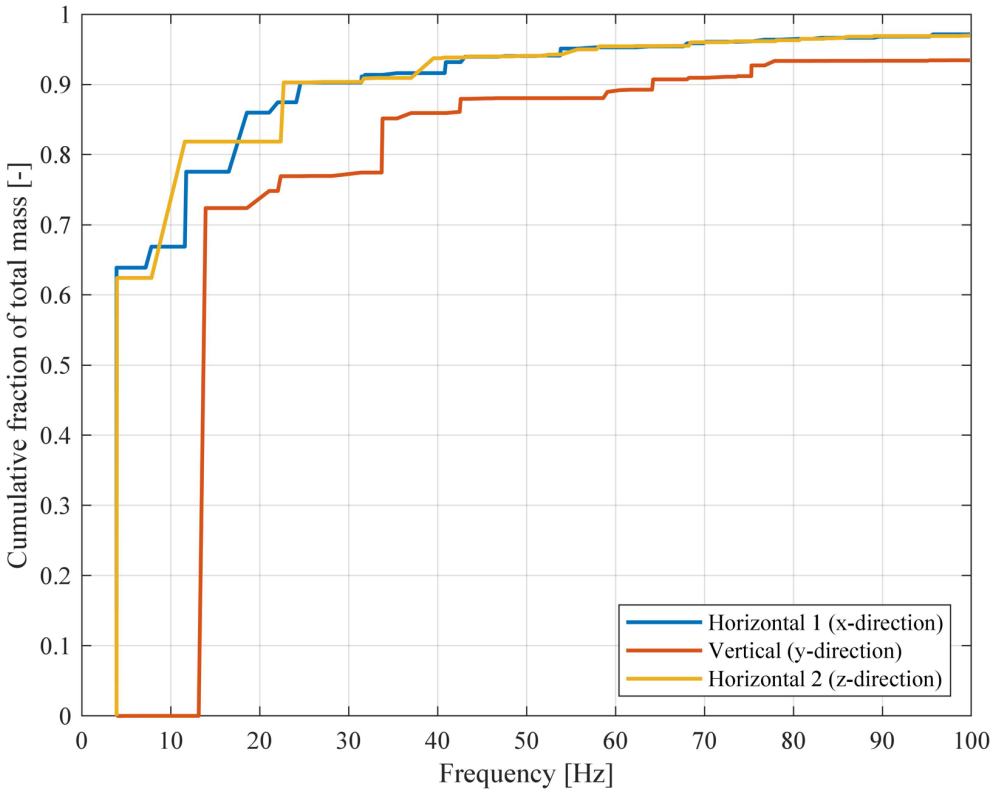

Figure 4-1 Obtained eigenfrequencies of the simplified containment structure in Example 1 together with the cumulative effective mass expressed as the fraction of the total mass of the model.

As can be seen in the figure, the modal masses taken into account in the analysis reach the recommended threshold of 90 % in all three directions. Moreover, it can be observed that there is one dominant mode in each direction. Each of these modes contributes to the cumulative effective mass with approximately 62-72 % of the total mass. The mode shapes of these three modes are shown in Figure 4-2, Figure 4-3 and Figure 4-4.

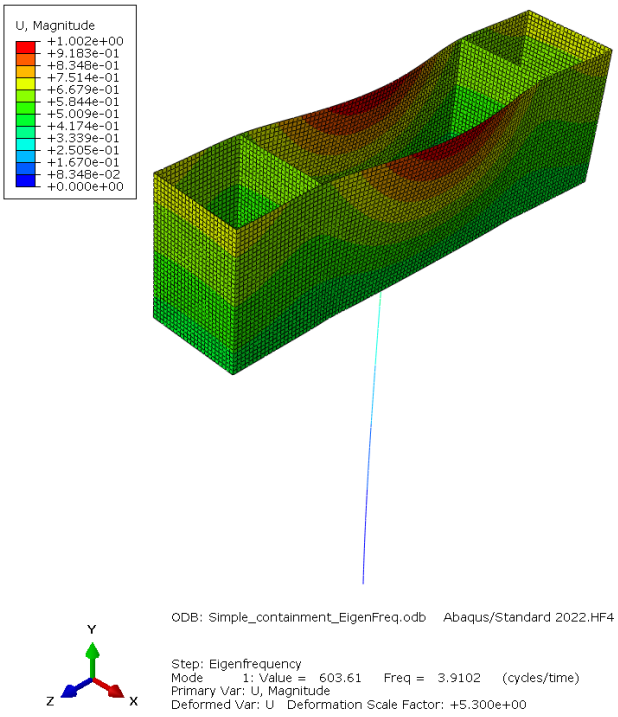

Figure 4-2 Dominant mode in horizontal direction 1 (H1) with a frequency of 3.91 Hz. The contour plot shows normalized displacements by mass.

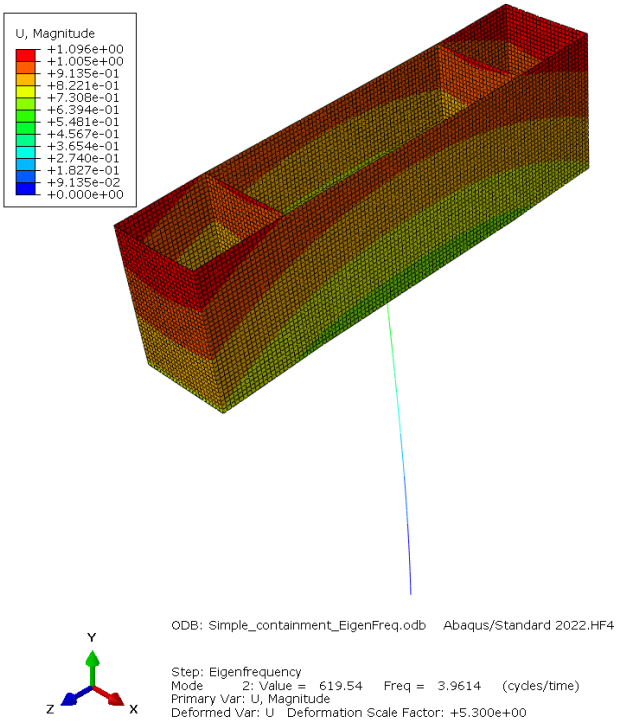

Figure 4-3 Dominant mode in horizontal direction 2 (H1) with a frequency of 3.96 Hz. The contour plot shows normalized displacements by mass.

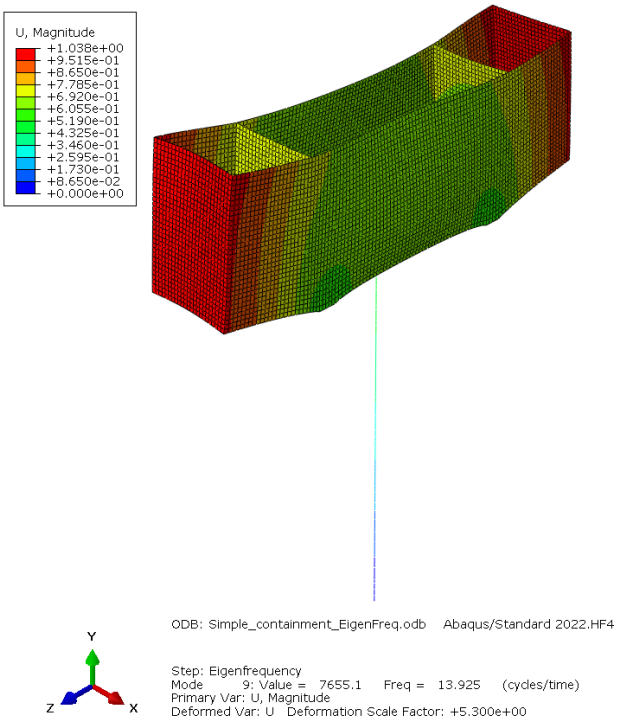

Figure 4-4 Dominant mode in vertical direction (V) with a frequency of 13.925 Hz. The contour plot shows normalized displacements by mass.

4.1.2 Floor Response Spectra

Floor response spectra (FRS) are developed in two selected nodes of the structure using the two investigated DSSMs and the results from the THA. The locations of the two nodes are shown with red dots in Figure 4-5.

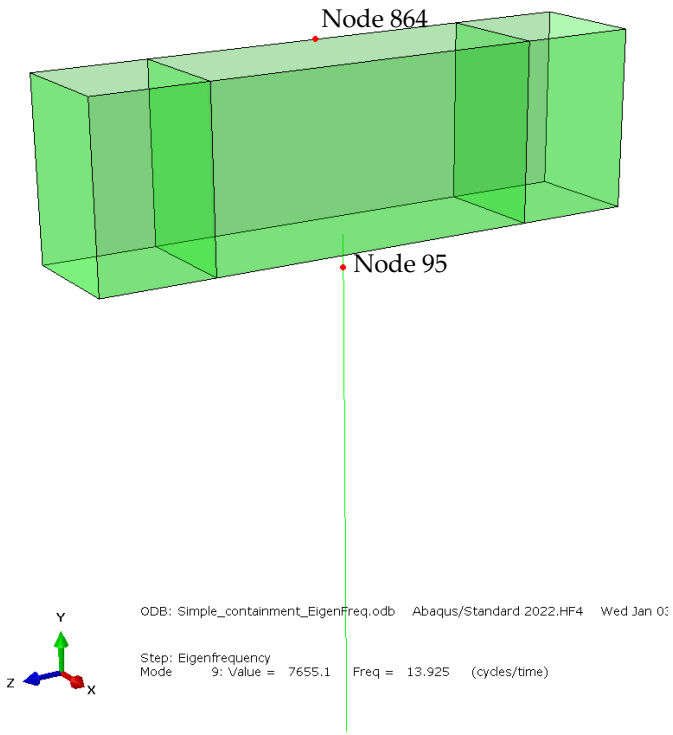

Figure 4-5 Locations of the two selected nodes for development of FRS.

In the reminder of this section, horizontal directions H1 and H2 refer to the x-direction and z-direction in Figure 4-5, respectively, whereas the vertical direction V refers to the y-direction.

The obtained FRS in both horizontal directions and the vertical direction for node 95 using the three methods are plotted in Figure 4-6, Figure 4-7 and Figure 4-8. Note that the thin coloured lines in the plots show the FRS for each analysed set of acceleration time series, and that the thick black line is the average of these FRS.

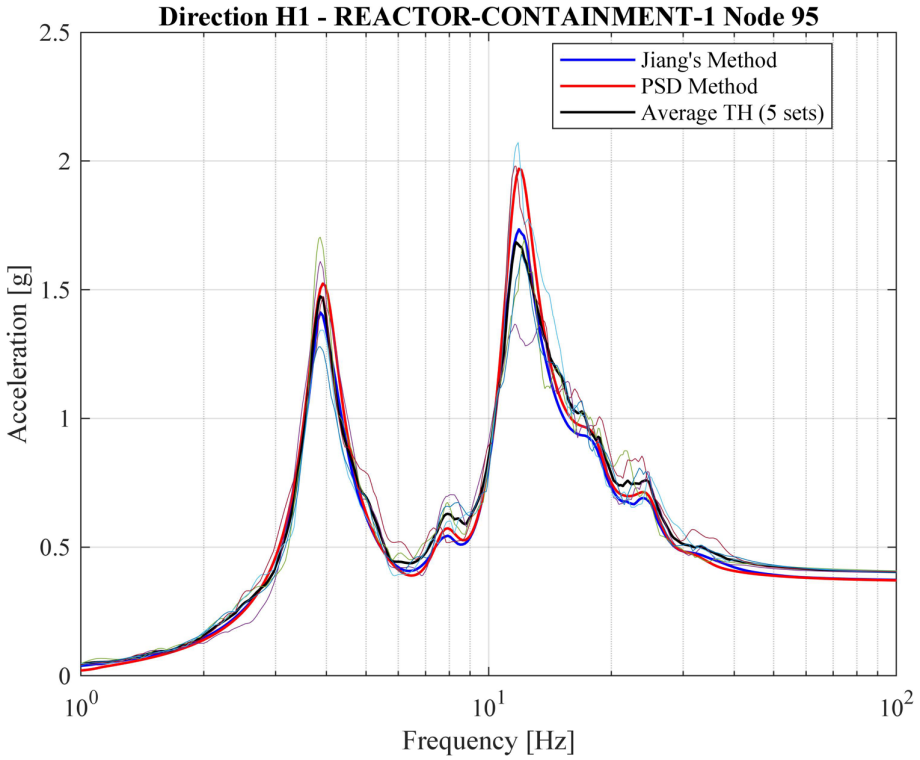

Figure 4-6 Comparison of FRS generated by DSSMs and THA in node 95, direction H1. The thin coloured lines show the FRS for each set of acceleration time series. The thick black line is the average of the THA.

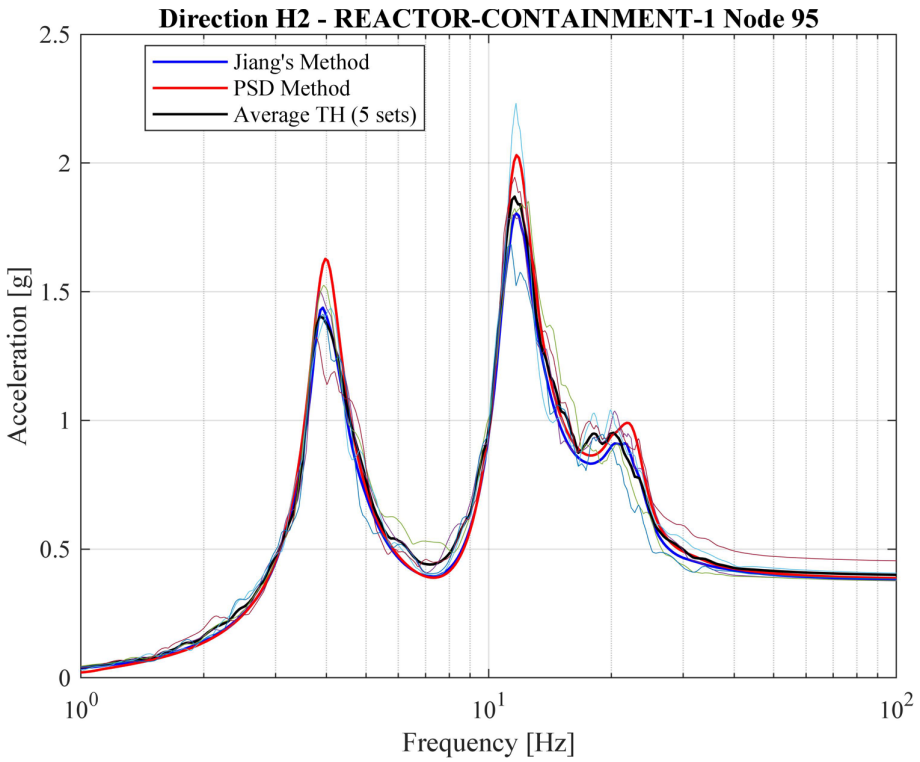

Figure 4-7 Comparison of FRS generated by DSSMs and THA in node 95, direction H2. The thin coloured lines show the FRS for each set of acceleration time series. The thick black line is the average of the THA.

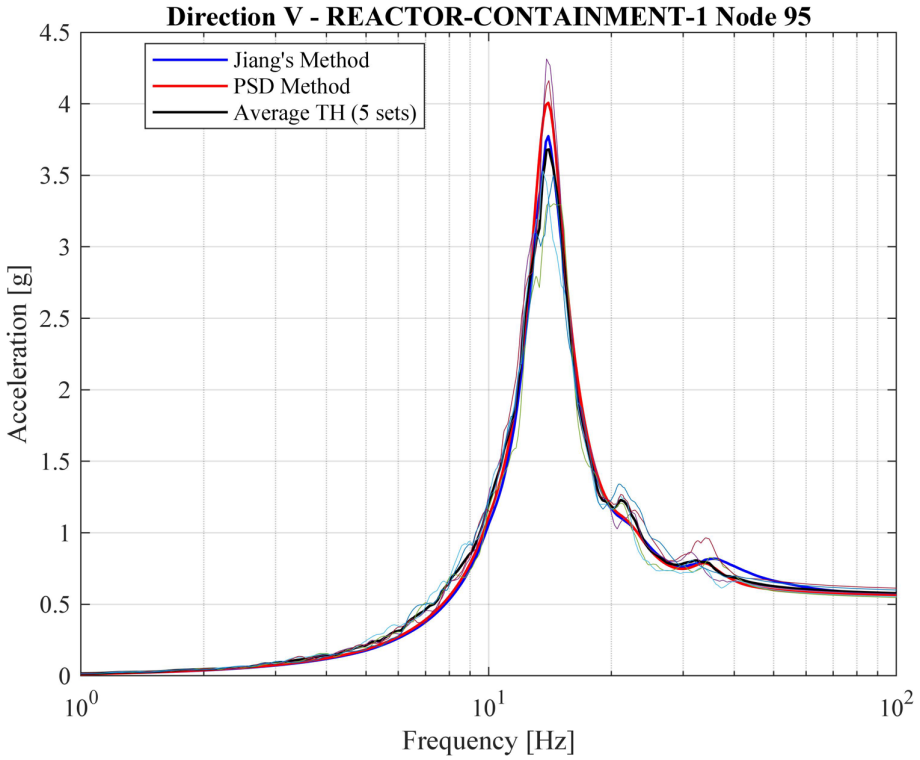

Figure 4-8 Comparison of FRS generated by DSSMs and THA in node 95, direction V. The thin coloured lines show the FRS for each set of acceleration time series. The thick black line is the average of the THA.

Comparing the overall shape of the FRS, it can be seen that the overall agreement between the three methods is good. Another observation that can be made is that the scatter among the five sets of acceleration time series is quite large, especially at the higher peaks. This highlights the importance of including more than one set of acceleration time series when conducting time history analysis of the earthquake response. Studying closer the individual peaks reveals that the results from Jiangs's method and the average of the time histories comply rather well. The PSD method tends to overestimate the peaks as compared to the average FRS generated by THA. The obtained response is though within the scatter of the individual time history analyses except at the first peak in direction H2, see Figure 4-7. A probable explanation to this observation is that the PSD method yields the steady-state response of the structure. For earthquakes with short periods of strong motion, such as the Swedish earthquake, a steady-state response might not be reached due to the dynamic inertia of the structure. This inertial effect is accounted for in time history analysis. Hence, the overestimation at the peaks in the FRS obtained by the PSD method compared to average FRS from the THA and the FRS from Jiang's method. This tendency of the PSD method should though be reduced or may even vanish for earthquakes with longer periods of strong motion. The FRS obtained using Jiang's method falls both slightly above and below the time history results at the peaks. At all major peaks, the FRS response are though within the scatter of the time history analyses.

The obtained FRS in both horizontal directions and the vertical direction for node 864 using the three methods are plotted in Figure 4-9, Figure 4-10 and Figure 4-11.

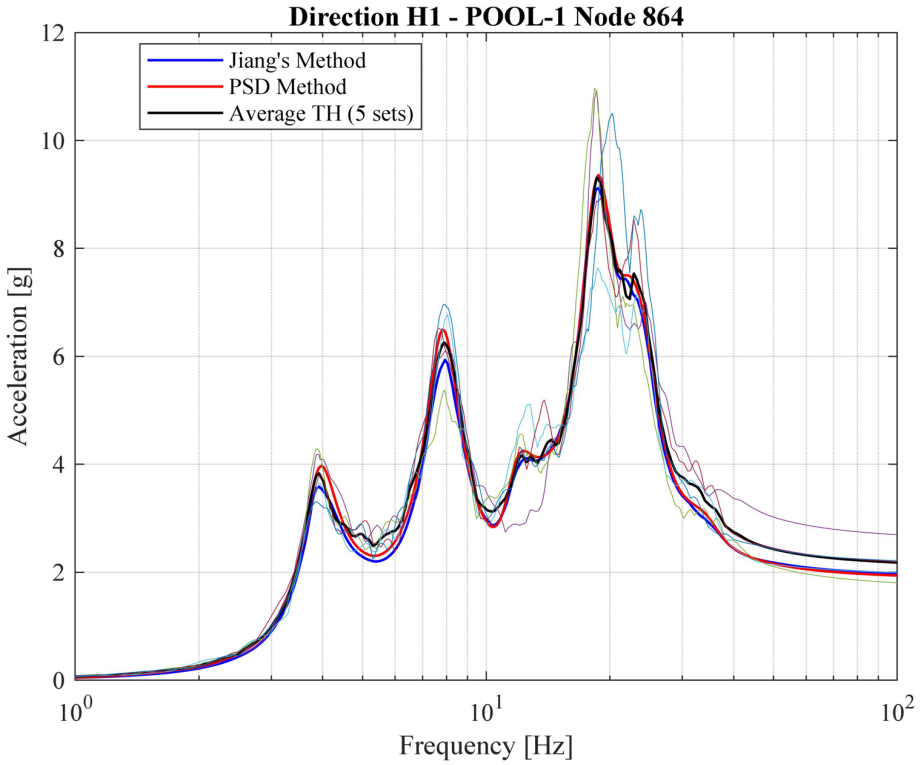

Figure 4-9 Comparison of FRS generated by DSSMs and THA in node 864, direction H1. The thin coloured lines show the FRS for each set of acceleration time series. The thick black line is the average of the THA.

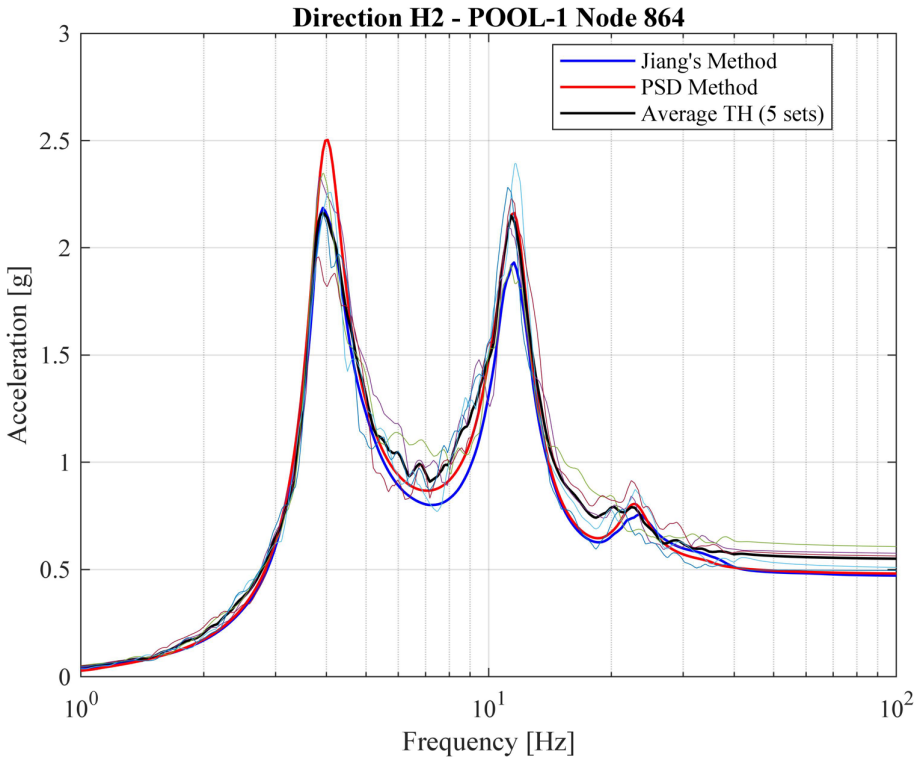

Figure 4-10 Comparison of FRS generated by DSSMs and THA in node 864, direction H2. The thin coloured lines show the FRS for each set of acceleration time series. The thick black line is the average of the THA.

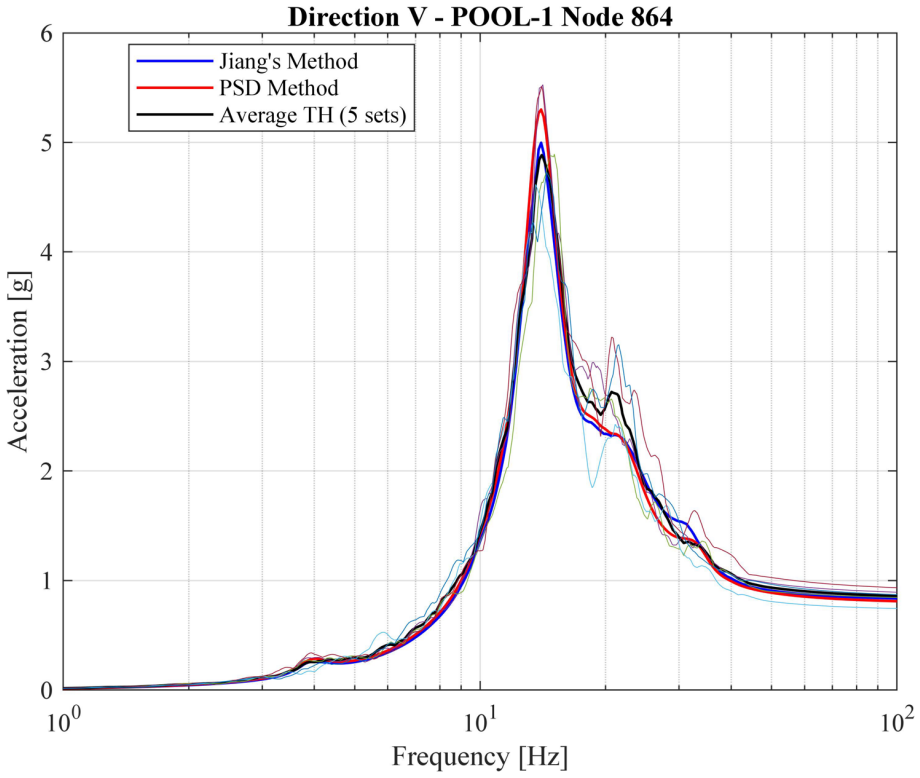

Figure 4-11 Comparison of FRS generated by DSSMs and THA in node 864, direction V. The thin coloured lines show the FRS for each set of acceleration time series. The thick black line is the average of the THA.

As for node 95, the overall shape of the obtained FRS agree well between the three methods. At some peaks the PSD method exceeds the response given by the other two methods, see e.g. the first peak in direction H2. However, the overall compliance with the other two methods at the peaks is better than in node 95. It is only at the first peak in direction H2 that the PSD method overshoot the scatter of the time history analyses. In direction H1, the three peaks in the FRS obtained using Jiang's method are smaller compared to the average time history FRS. The largest deviation occurs at the first peak where the acceleration response is 6.5 % lower. In direction H2, the response is only lower at the second peak, where the acceleration is approximately 10 % smaller compared to the time history response. All obtained peaks in the FRS using Jiang's method do though fall inside the scatter of the time history analyses.

As described in section 3.3, the tRS used for the two horizontal directions was obtained as the average tRS based on all ten horizontal acceleration time series. In the work by Jiang et al. [4], more than 30 sets of time series were used to evaluate the tRS and also for obtaining the average time history response. Hence, the number of used sets in the current study is probably too small to obtain the actual average time history response as well as a generic tRS for the design GRS in the horizontal and vertical directions. Following these observations, it was tested to evaluate separate tRS in the two horizontal directions based on the same acceleration time series applied in each individual direction in the time history analyses. The obtained FRS based on the two separate horizontal tRS in node 864 for directions H1 and H2 are plotted in Figure 4-12 and Figure 4-13.

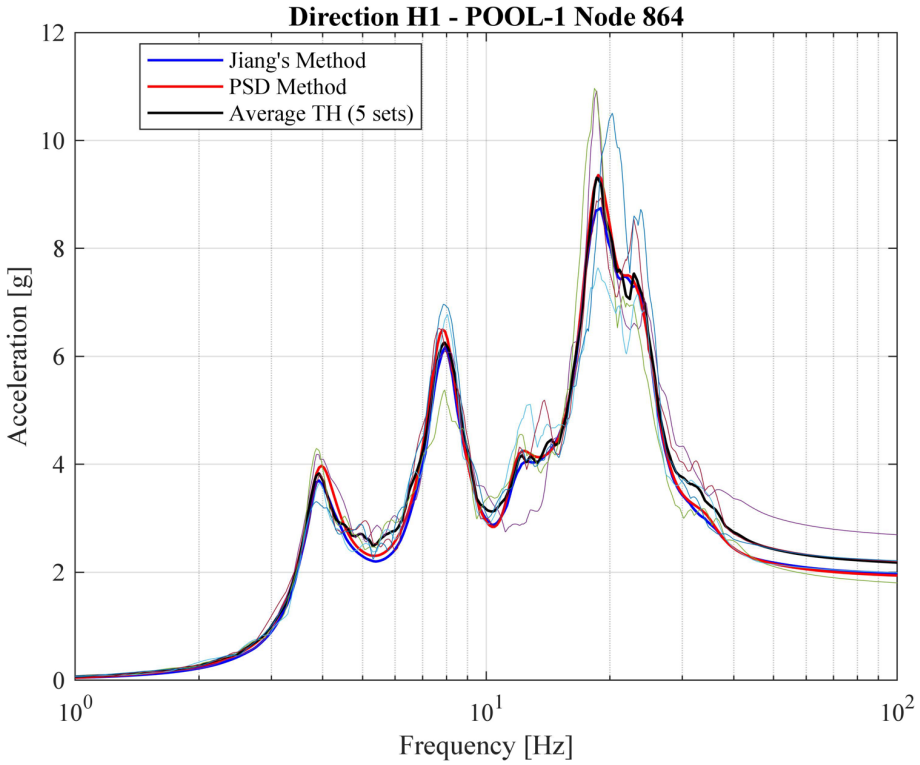

Figure 4-12 Comparison of FRS generated by DSSMs and THA in node 864, direction H1, using separate tRS in directions H1 and H2. The thin coloured lines show the FRS for each set of acceleration time series. The thick black line is the average of the THA.

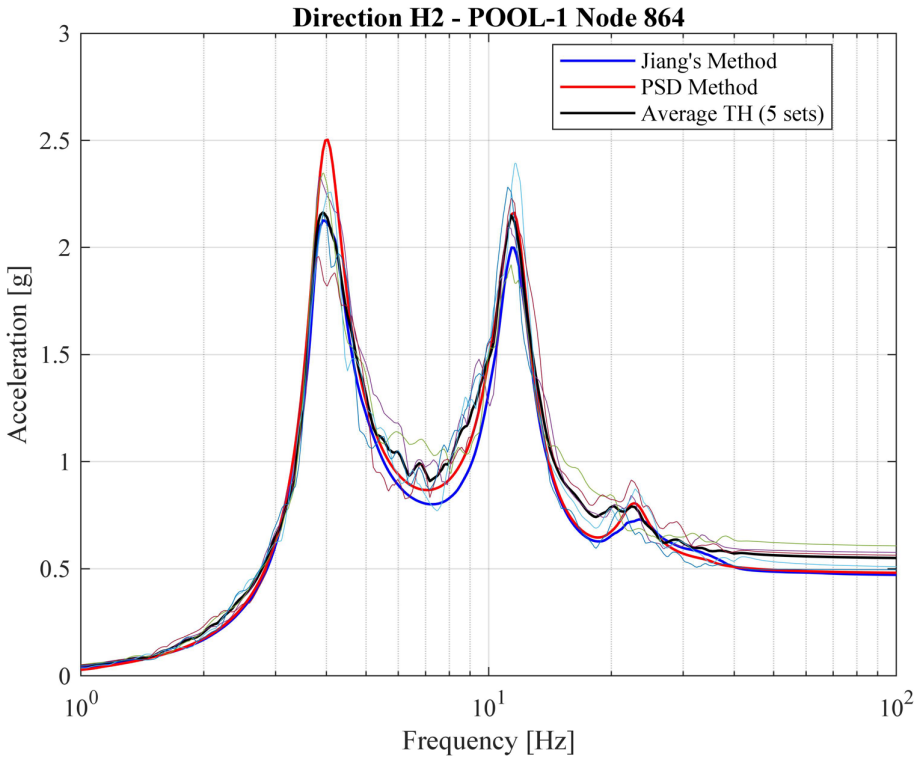

Figure 4-13 Comparison of FRS generated by DSSMs and THA in node 864, direction H2, using separate tRS in directions H1 and H2. The thin coloured lines show the FRS for each set of acceleration time series. The thick black line is the average of the THA.

As can be seen in the figures, the agreement between the two first peaks in direction H1 increases. In the third peak, an increased difference is instead observed, but the response acceleration is still well within the limits of time history response scatter. The difference between the two methods is approximately 6 % at the third peak in Figure 4-12. In direction H2, the difference at the second peak has decreased to approximately 7 %, whereas it has slightly increased at the first peak. The acceleration response at both peaks is well within the limits of the time history response scatter. The FRS in the horizontal directions in node 95 are also improved when using separate tRS in the two horizontal directions. The obtained FRS in node 95 for direction H2 is shown in Figure 4-14.

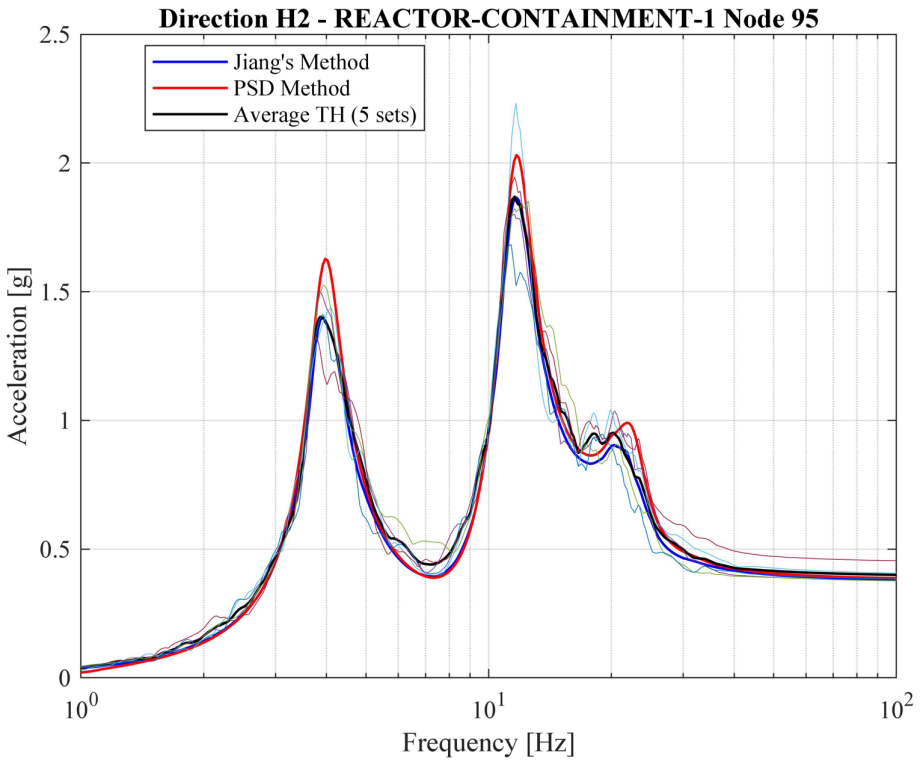

Figure 4-14 Comparison of FRS generated by DSSMs and THA in node 95, direction H2, using separate tRS in directions H1 and H2. The thin coloured lines show the FRS for each set of acceleration time series. The thick black line is the average of the THA.

As can be observed in the figure, the FRS response at the two peaks become almost identical for Jiang's method and the time series method. In summary, the results indicate that the number of sets used in the evaluation of the tRS in Figure 3-11 and Figure 3-12 is too small to obtain a generic tRS for the considered design GRS in the horizontal and vertical directions. The same also applies to the average FRS obtained from the time history analyses, where a larger number of sets is necessary to obtain the actual average time history FRS with regard to the used design GRS.

Results from calculated relative differences of the FRS response obtained from the DSSMs and the five THA compared to the average TH value in each direction of the two studied nodes are compiled in Table 4-1. The maximum values around each major FRS peak are used in the evaluation of the differences since the peak

frequencies slightly vary between the methods. The corresponding differences between peaks are less important and, thus, not evaluated. The presented values correspond to the average and median relative difference of all major peaks in the FRS. Note that separate values are presented for Jiang's method using the tRS based on all ten horizontal time series and using separate tRS for the two horizontal directions. In the table, the former case is denoted *Jiang All H*, whereas the latter is denoted *Jiang Dir H*. In addition, the average and median coefficient of variation in the scatter of the TH results at the same peaks are presented.

Table 4-1 Compilation of calculated relative differences in FRS response obtained from the DSSMs and the five THA compared to the average TH response at all major peaks in Example 1. Additionally, relative standard deviations (coefficient of variation) in the scatter of the TH results at the same peaks are presented.

	TH	Jiang All H**	Jiang Dir H**	PSD
Average relative difference to average TH [%]	13.1*	3.9	2.3	7.9
Median relative difference to average TH [%]	12.9*	3.0	1.4	8.6
Average coefficient of variation TH [%]	10.7	-	-	-
Median coefficient of variation TH [%]	10.5	-	-	-

*The relative difference at each individual peak is first evaluated by calculating the average of the relative difference of the min and max TH response to the average TH response. The values presented in the table are then obtained by calculating the average and median of the averaged relative differences at all major peaks in all FRS.
**Column *Jiang All H* presents results from Jiangs's method using a single tRS based on all ten horizontal time series, whereas *Jiang Dir H* presents results using separate tRS in the two horizontal directions.

Based on the observations in Example 1, the agreement between the FRS obtained using the three different methods in the current example is judged to be adequate enough to use any of them in various design situations.

4.2 EXAMPLE 2 – GENERIC SERVICE BUILDING

4.2.1 Eigenfrequencies

The obtained eigenfrequencies of the structure up to 200 Hz are plotted in Figure 4-15 together with the cumulative effective mass in each main direction of the model. Note that the effective mass is expressed as the fraction of the total mass ($1.48 \cdot 10^6$ kg) of the model. The total number of modes is 915, whereas the number of modes up to 100 Hz is 353.

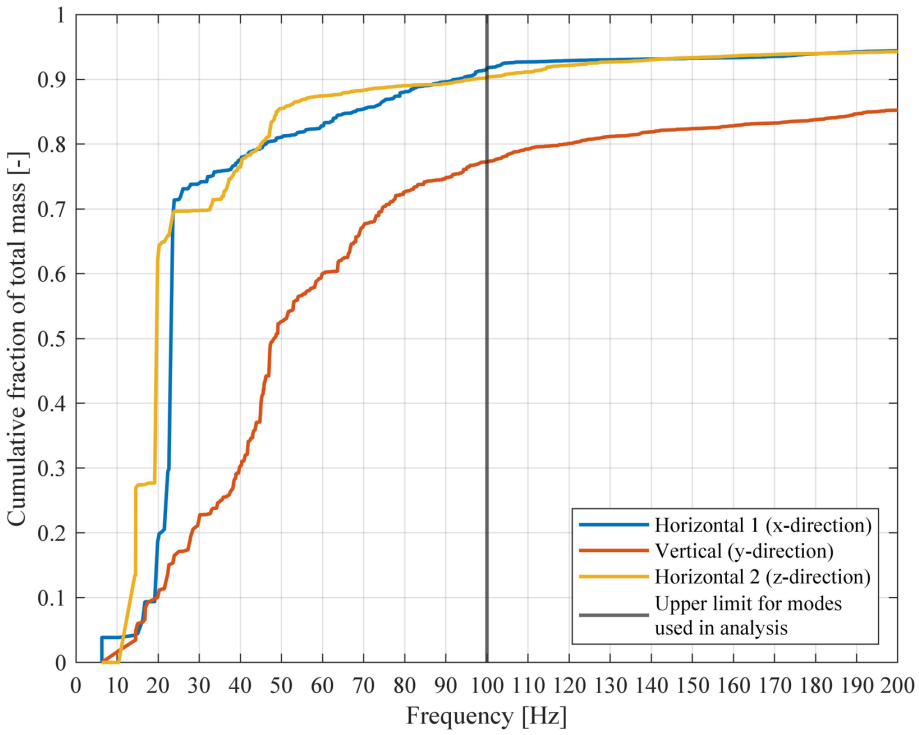

Figure 4-15 Obtained eigenfrequencies of the generic service building in Example 2 together with the cumulative effective mass expressed as the fraction of the total mass of the model.

As can be seen in the figure, the cumulative modal masses reach the recommended threshold of 90 % in the two horizontal directions at approximately 100 Hz. For the vertical direction, the threshold value is not reached even at 200 Hz. This is because the service building is stiff in its vertical direction. Hence, the significance of the modes above 100 Hz to the total response of the structure is limited. Furthermore, in Eurocode 8 [39] section 4.3.3.3.1(3), an alternative requirement for determining the number of modes to include in an analysis is given. It is stated that all modes with effective modal masses greater than 5 % of the total mass should be taken into account. As seen in the figure, there are no modes with frequency higher than 100 Hz that has an effective mass greater than 5 %. Hence, only the modes up to 100 Hz are included in the performed analyses of the service building.

For the two horizontal directions, it can be observed that there is one dominant mode in each direction. These modes contribute to the cumulative effective mass with approximately 39 % and 34 % of the total mass in horizontal direction H1 and H2, respectively. In vertical direction, the contribution to the cumulative effective mass from a single mode is not as dominant. The mode shapes of the two dominant modes in the horizontal directions are shown in Figure 4-16 and Figure 4-17. For the vertical direction, an example of one of the more significant modes is presented in Figure 4-18.

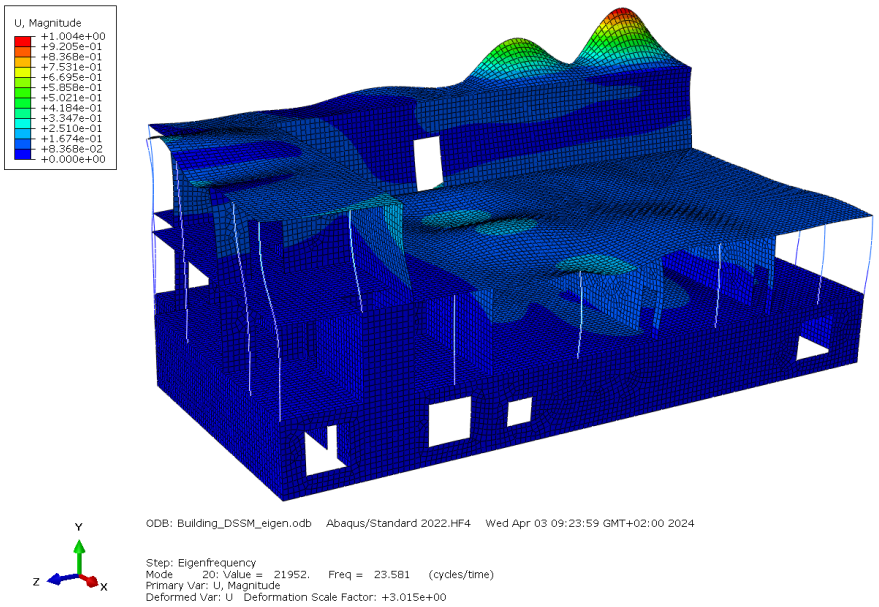

Figure 4-16 Dominant mode in horizontal direction 1 (H1) with a frequency of 23.58 Hz. The contour plot shows normalized displacements by mass.

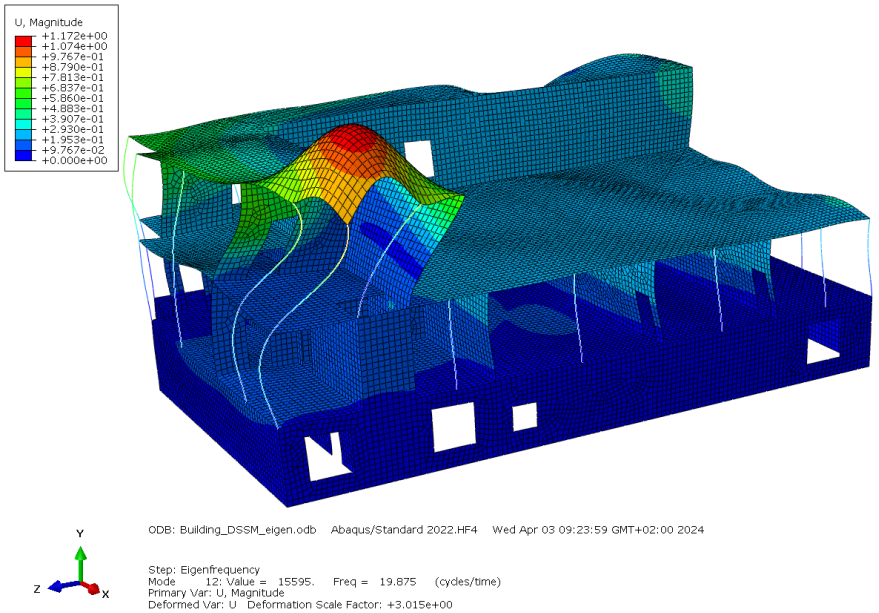

Figure 4-17 Dominant mode in horizontal direction 2 (H2) with a frequency of 19.88 Hz. The contour plot shows normalized displacements by mass.

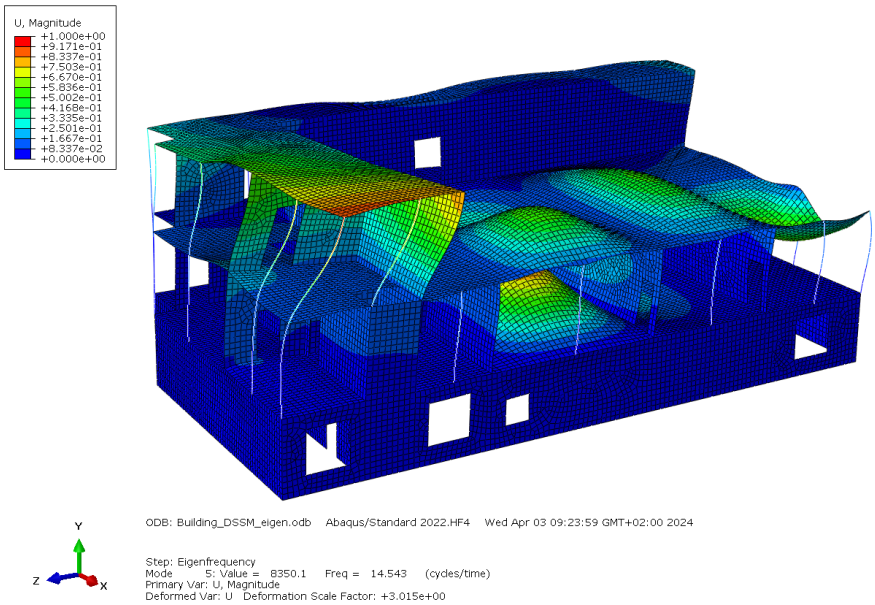

Figure 4-18 Example of significant mode in vertical direction (V) with a frequency of 14.54 Hz. The contour plot shows normalized displacements by mass.

4.2.2 Floor Response Spectra

Floor response spectra (FRS) are developed at three selected nodes in the building using the two investigated DSSMs and the results from the THA. The locations of the three nodes are shown with red dots in

Figure 4-19.

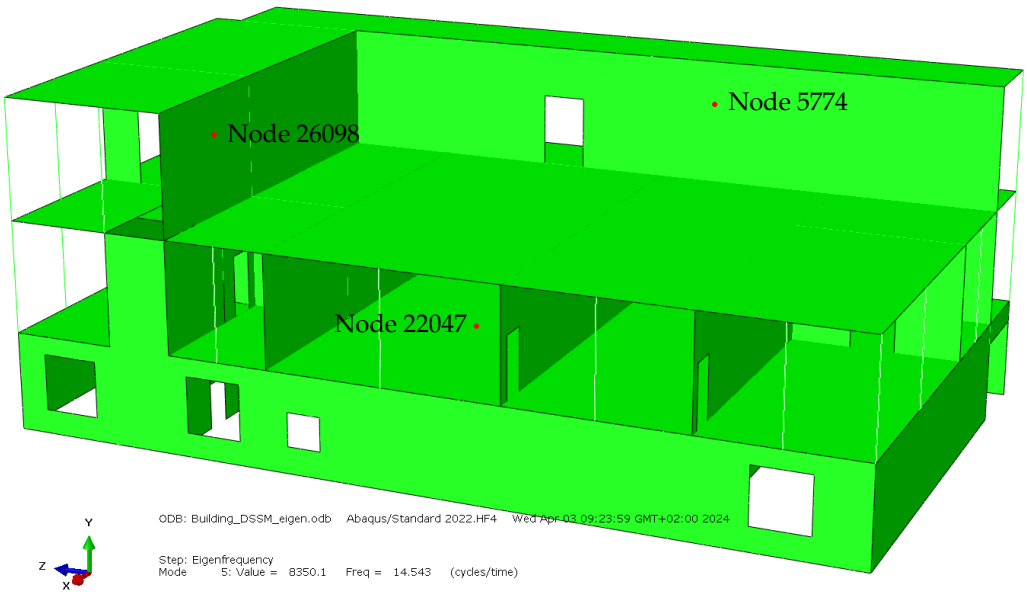

Figure 4-19 Locations of the three selected nodes for evaluation of FRS.

In the reminder of the section, horizontal directions H1 and H2 refer to the x-direction and z-direction in Figure 4-19, respectively, whereas the vertical direction V refers to the y-direction.

The obtained FRS in both horizontal directions and the vertical direction at node 5774, using the three methods, are plotted in Figure 4-20, Figure 4-21 and Figure 4-22. Note that the thin coloured lines in the plots show the FRS for each analysed set of acceleration time series, and the thick black line is the average of these FRS.

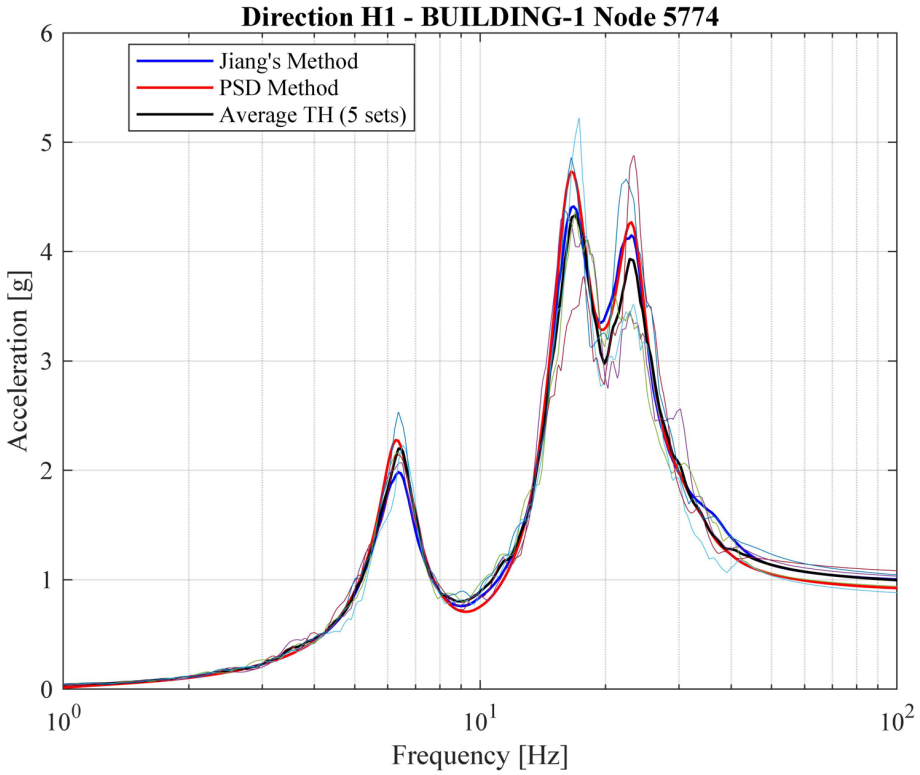

Figure 4-20 Comparison of FRS generated by DSSMs and THA in node 5774, direction H1. The thin coloured lines show the FRS for each set of acceleration time series. The thick black line is the average of the THA.

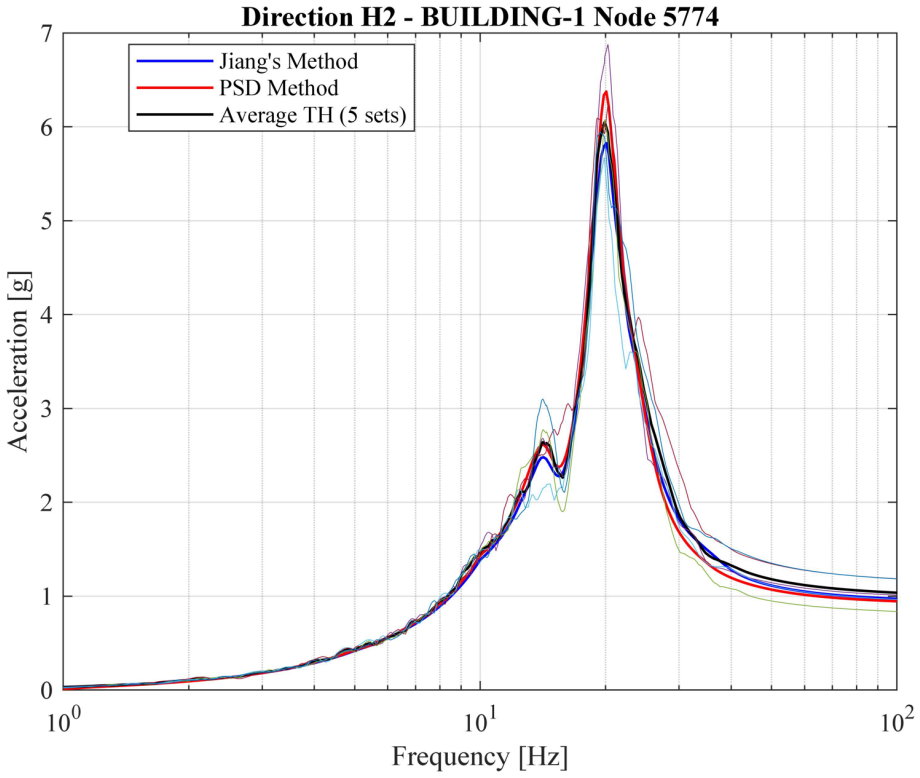

Figure 4-21 Comparison of FRS generated by DSSMs and THA in node 5774, direction H2. The thin coloured lines show the FRS for each set of acceleration time series. The thick black line is the average of the THA.

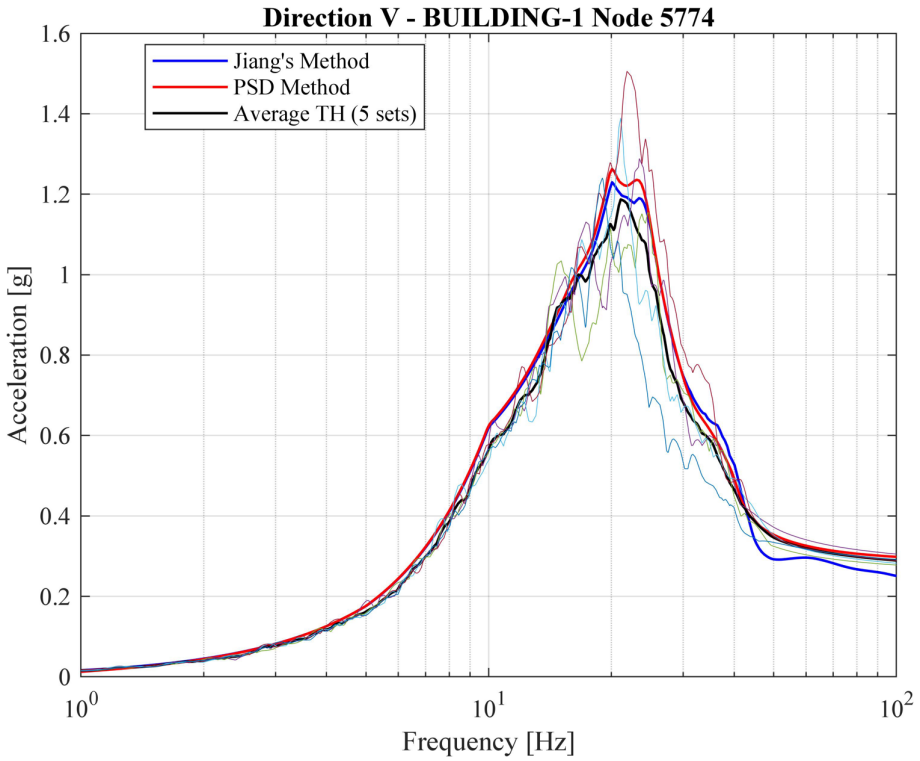

Figure 4-22 Comparison of FRS generated by DSSMs and THA in node 5774, direction V. The thin coloured lines show the FRS for each set of acceleration time series. The thick black line is the average of the THA.

Comparing the overall shape of the FRS, it can be seen that the agreement between the three methods is good. As in Example 1, the PSD method has a tendency to exceed the peak response as compared to the average FRS generated by time history. The obtained response is though within the scatter of the individual time history analyses in all directions. A possible explanation to this overestimation by the PSD method is given in section 4.1.2. The FRS obtained using Jiang's method falls both slightly above and below the average time history FRS at the peaks. However, at the first peak in direction H1, the response obtained using Jiang's DSSM is smaller than the lower limit of the time history response scatter. Compared to the average time history FRS, Jiang's method yields approximately a 10 % smaller acceleration. As described in section 4.1.2, the number of sets used in the evaluation of the tRS in Figure 3-11 and Figure 3-12 is too small to obtain a generic tRS for the considered design GRS in the horizontal and vertical directions. The same also applies to the average FRS obtained from the THA, where a larger number of sets is necessary to obtain the actual average time history FRS with regard to the used design GRS. Using the tRS evaluated separately for the two horizontal directions from Example 1 yields better agreement with the average FRS generated by THA, see Figure 4-23.

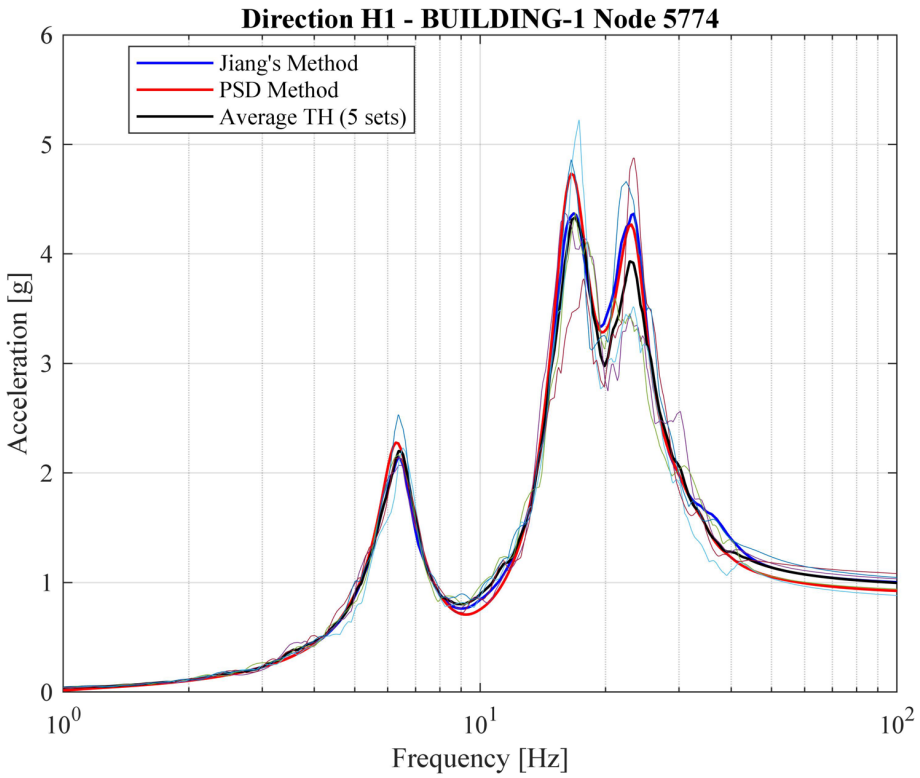

Figure 4-23 Comparison of FRS generated by DSSMs and THA in node 5774, direction H1, using separate tRS in directions H1 and H2. The thin coloured lines show the FRS for each set of acceleration time series. The thick black line is the average of the THA.

The response acceleration at the first peak in the figure now only differs by approximately 2.7 %, and also falls within the limits of the time history response scatter at all three peaks. The agreement at the peaks in the other directions is also

improved when using the separate horizontal tRS. No further plots at the current node are though presented in the report, but can be found in Appendix A:.

The obtained FRS in both horizontal directions and the vertical direction at node 26098 using the three methods are plotted in Figure 4-24, Figure 4-25 and Figure 4-26.

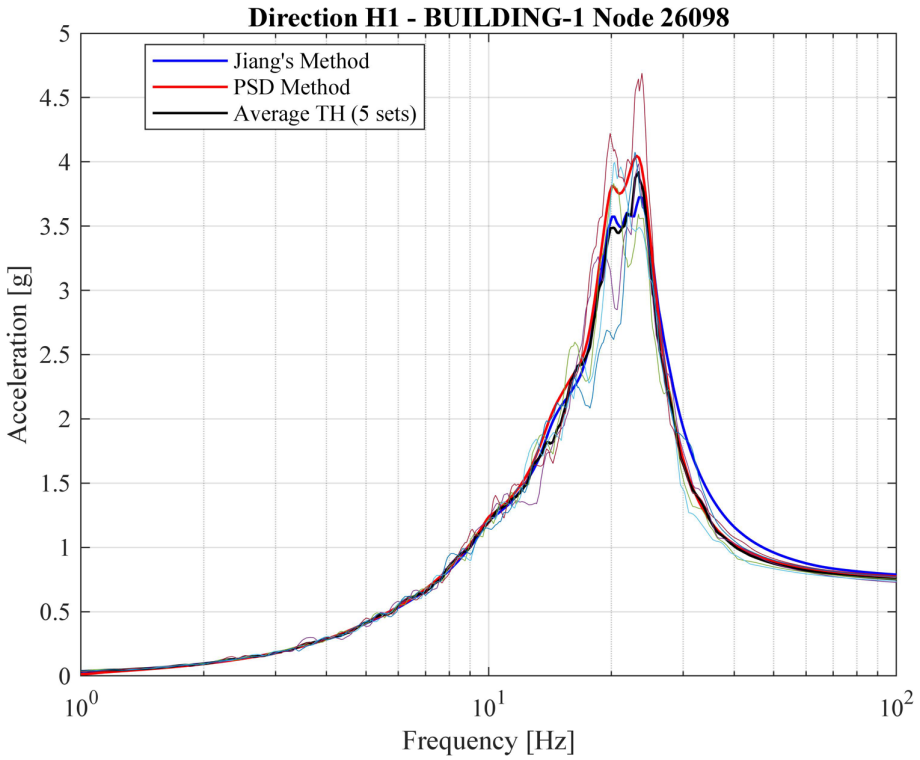

Figure 4-24 Comparison of FRS generated by DSSMs and THA in node 26098, direction H1. The thin coloured lines show the FRS for each set of acceleration time series. The thick black line is the average of the THA.

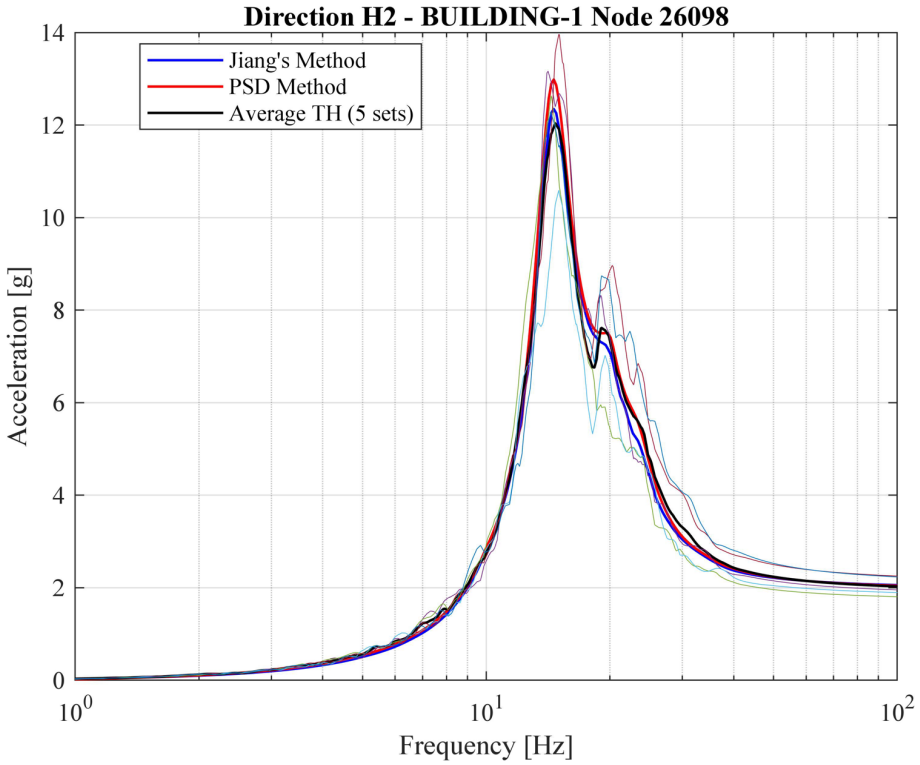

Figure 4-25 Comparison of FRS generated by DSSMs and THA in node 26098, direction H2. The thin coloured lines show the FRS for each set of acceleration time series. The thick black line is the average of the THA.

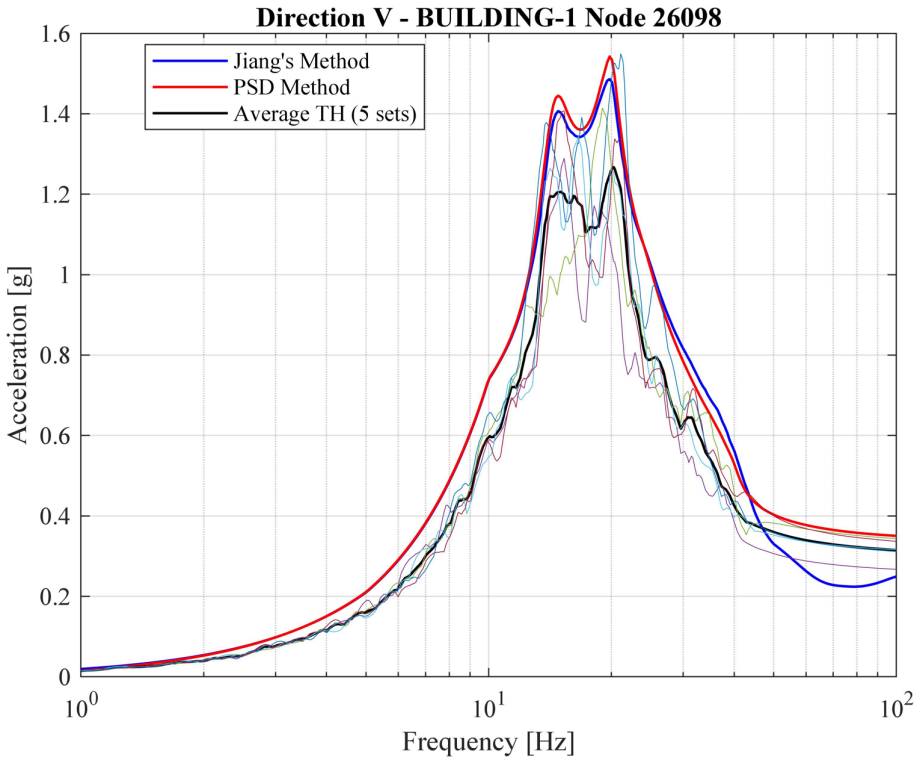

Figure 4-26 Comparison of FRS generated by DSSMs and THA in node 26098, direction V. The thin coloured lines show the FRS for each set of acceleration time series. The thick black line is the average of the THA.

As for the previously studied node, the overall shape of the obtained FRS agree well between the three methods. The PSD method overestimates the acceleration response of the two other methods at all peaks. In the two horizontal directions, the accelerations are though within the limits of the time history response scatter. The FRS obtained using Jiang's method falls both slightly above and below the average time history FRS at the peaks in the horizontal directions, but are within the limits of the scatter. The largest difference in the horizontal directions occur for the peak in direction H1, where Jiang's method yields a 5.1 % lower acceleration compared to the average time history FRS. Using the separate tRS for the two horizontal directions, Jiang's method instead yields a 2.6 % larger acceleration compared to the average time history FRS at the peak, see Figure 4-27.

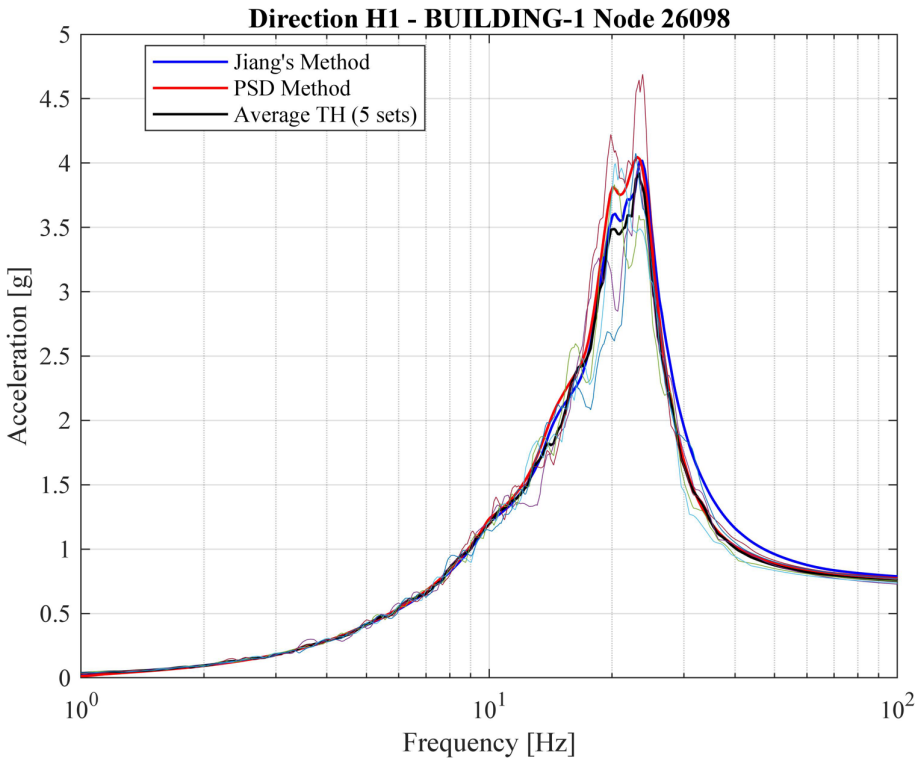

Figure 4-27 Comparison of FRS generated by DSSMs and THA in node 26098, direction H1, using separate tRS in directions H1 and H2. The thin coloured lines show the FRS for each set of acceleration time series. The thick black line is the average of the THA.

In the vertical direction, both the PSD method and Jiang's method overshoot the average time history FRS, and also falls slightly outside the upper limit of the scatter. Applying the separate horizontal tRS in Jiang's method leads to almost identical results. Studying the results in Figure 4-22, a similar trend with both DSSMs overshooting the average time history FRS at the peak is observed. It has not been possible to find an explicit explanation to these observations, but they may also be a consequence of the limited number of time series used in this study.

The obtained FRS in both horizontal directions and the vertical direction at node 22047 using the three methods are plotted in Figure 4-28, Figure 4-29 and Figure

4-30.

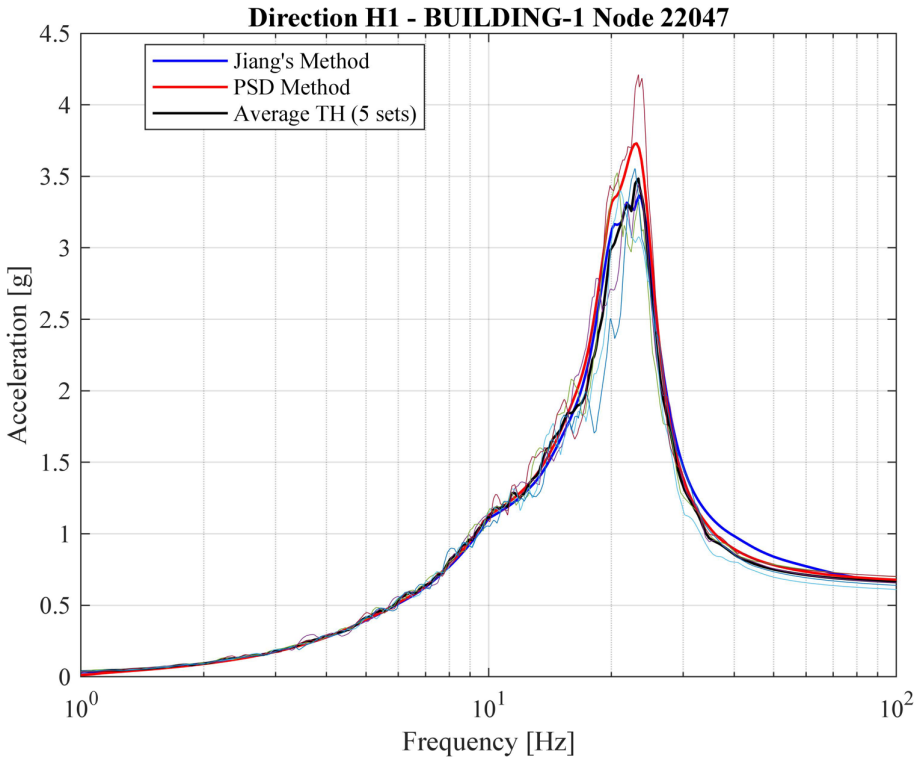

Figure 4-28 Comparison of FRS generated by DSSMs and THA in node 22047, direction H1. The thin coloured lines show the FRS for each set of acceleration time series. The thick black line is the average of the THA.

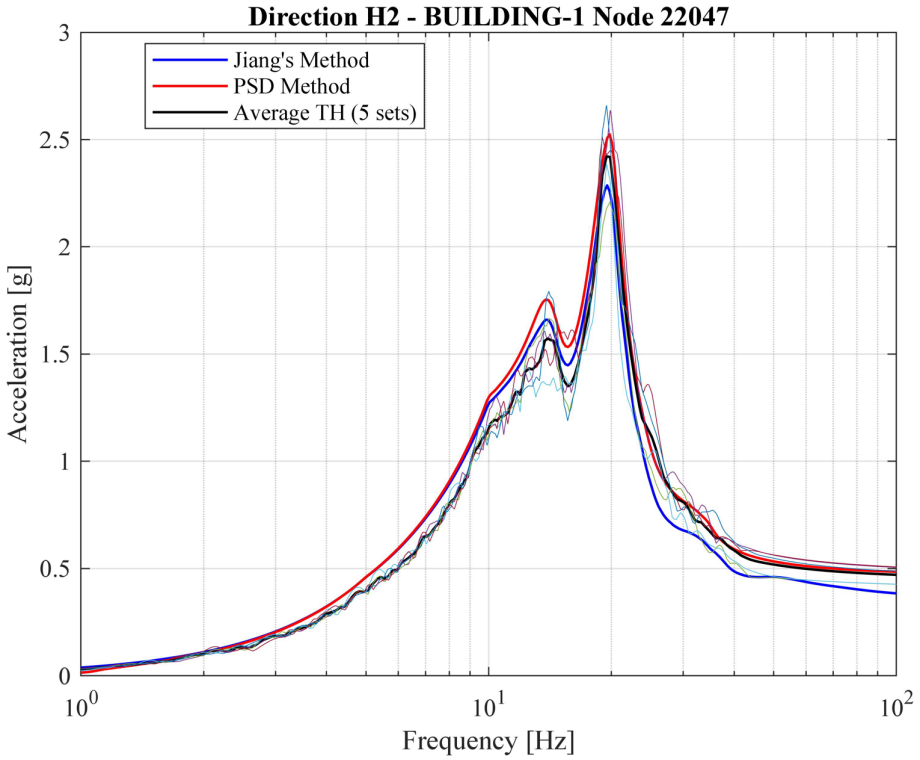

Figure 4-29 Comparison of FRS generated by DSSMs and THA in node 22047, direction H2. The thin coloured lines show the FRS for each set of acceleration time series. The thick black line is the average of the THA.

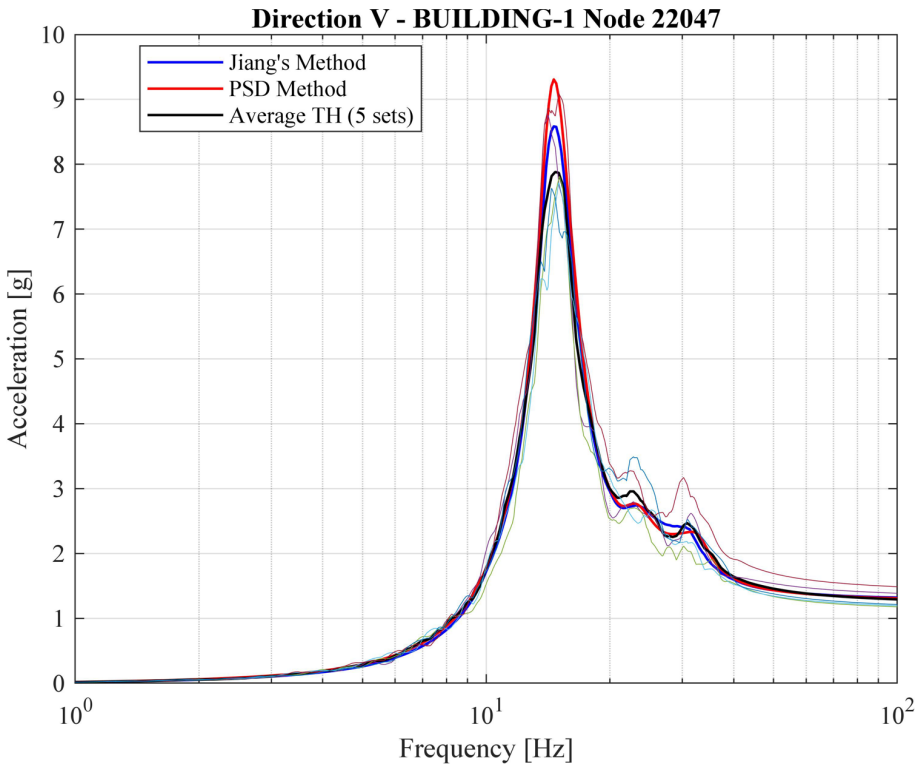

Figure 4-30 Comparison of FRS generated by DSSMs and THA in node 22047, direction V. The thin coloured lines show the FRS for each set of acceleration time series. The thick black line is the average of the THA.

Referring back to Figure 4-19, showing the locations of the selected nodes, it can be seen that node 22047 is located at midspan in one of the concrete slabs on the second floor. Hence, the largest acceleration response occurs in the vertical direction. The other observations that can be made in the obtained FRS at node 22047 using the three methods are similar to the two previously studied nodes, and are thus not further commented.

Results from calculated relative differences of the FRS response obtained from the DSSMs and the five THA compared to the average TH response at all major response peaks in the three studied nodes are compiled in Table 4-2. The presented values correspond to the average and median relative difference of all major peaks in the FRS. Note that separate values are presented for Jiang's method using the tRS based on all ten horizontal time series and using separate tRS for the two horizontal directions. In the table, the former case is denoted *Jiang All H*, whereas the latter is denoted *Jiang Dir H*. In addition, the average and median coefficient of variation in the scatter of the TH results at the same peaks are presented.

Table 4-2 Compilation of calculated relative differences in FRS response obtained from the DSSMs and the five THA compared to the average TH response at all major peaks in Example 2. Additionally, relative standard deviations (coefficient of variation) in the scatter of the TH results at the same peaks are presented.

	TH	Jiang All H**	Jiang Dir H**	PSD
Average relative difference to average TH [%]	14.4*	6.6	6	9
Median relative difference to average TH [%]	15.1*	5.4	3.4	7.8
Average coefficient of variation TH [%]	11.4	-	-	-
Median coefficient of variation TH [g]	11.7	-	-	-

*The relative difference at each individual peak is first evaluated by calculating the average of the relative difference of the min and max TH response to the average TH response. The values presented in the table are then obtained by calculating the average and median of the averaged relative differences at all major peaks in all FRS.

**Column *Jiang All H* presents results from Jiangs's method using a single tRS based on all ten horizontal time series, whereas *Jiang Dir H* presents results using separate tRS in the two horizontal directions.

In summary, the results from Example 2 also show that the agreement between the FRS using the three methods is adequate enough to use any of them in various design situations.

4.3 SUMMARISING DISCUSSION

The FRS obtained using the three methods in the two studied examples show an overall good agreement in shape and acceleration response at the peaks. The results also clearly show that there is a significant scatter in the individual FRS

obtained from time history analyses, especially at the peaks, even though they were generated to match the same design GRS. The average and median coefficient of variation among all major response peaks in both studied examples are 11.2 % and 11.4 %, respectively. The corresponding coefficients of variations evaluated separately for each example are given in Table 4-1 and Table 4-2. This emphasizes the importance of using several sets of acceleration time series followed by averaging of the results when adopting this method to develop FRS. In ASCE 4-16 [2] it is recommended to use at least five sets of acceleration time series. The FRS evaluated using either of the two studied DSSMs are mostly within the scatter of the time history-based FRS.

Running THA is quite time consuming even for linear models since a rather small time step is required. As mentioned in section 3.4, ASCE 4-16 recommends to use a time step corresponding to 0.1 times the shortest period of interest. Hence, in the two examples, a time step of 0.001 s (1 ms) was used. Furthermore, to evaluate FRS from the time history results, large quantities of output data also need to be stored from the FE analysis. Using the two studied DSSMs, only a single eigenfrequency analysis of the structure is needed, which is significantly faster to run compared to a time history analysis. A comparison of the analysis time and quantities of data in the two examples is presented in Table 4-3.

Table 4-3 Comparison of analysis time and data quantities from the performed FE analyses. Note that the analysis time and data quantity for the time history analyses include all five sets of acceleration time series.

Example	Time history: Analysis time	Eigenfrequency: Analysis time	Time history: Data	Eigenfrequency: Data
Example 1	42 min	12 s	34 GB	40 MB
Example 2	4.4 h	83 s	88.3 GB	347 MB

As seen in the comparison, there is a large difference in both analysis time and data quantity. Even though the two models are rather small, quite substantial quantities of data are produced in the time history analyses. Storage of data is of course not a significant issue nowadays, but is still a factor to consider for larger models. Concerning the analysis time, the use of DSSMs can help to speed up the seismic design of SSCs, especially in situations where the designer needs to investigate several different design alternatives. It should be noted that the development of the FRS, once the results from the FE analysis have been obtained, is quick and usually is completed within a few seconds regardless of which method is used.

In Jiang's method, the tRS must be evaluated based on the design GRS at the site and each considered damping value. The process of evaluating the average tRS using Eq. (2-9) from several time series is quick, and only took a few seconds for the ten horizontal time series considered in the two examples. However, as mentioned in sections 4.1 and 4.2, the results indicate that the number of sets of acceleration time series is too small to obtain a generic tRS for the considered design GRS. The same also applies to the average FRS obtained from the time history analyses, where a larger number of sets is necessary to obtain the actual average time history FRS with regard to the used design GRS. In the work by Jiang et al. [4], at least 30 time series in each direction were used when evaluating the performance of their proposed method. Furthermore, it should be noted that the

tRS only need to be evaluated once for each site. However, the evaluation must be performed for each exceedance probability and damping value of interest.

At the FRS peaks, the PSD method tends to overestimate the acceleration response of the other two methods. A probable explanation is that the structures never reach a steady-state response due to the short duration time of the Swedish earthquake, see further explanation in section 4.1.2. Because of this, the PSD method generally yields more conservative accelerations at the FRS peaks. However, it should be noted that the peak response is most often still within the scatter of the THA in both examples. The effect from assuming stationarity when using Lalanne's expression for expected maximum is believed to be small, since the assumption is made both when finding the GRS-equivalent PSD and then in the opposite direction when calculating the FRS from the floor PSD. The effects at each stage are cancelling each other out to a large extent. In fact, the choice of duration T for the GRS-equivalent random vibration has no effect on the result at all. The only thing that is important is that you use the same duration, of course, when calculating the FRS. One could say that a GRS-equivalent stationary random vibration is replacing the true earthquake vibration, in an intermediate state, to facilitate efficient response and FRS calculation. The steady state assumption, however, is only made once in the response calculation, so that bias remains. The results from the presented examples show only moderate effects and, as mentioned before, the effect would be even smaller for earthquake vibration with longer duration. One can also see a larger effect for peaks at lower frequencies, for the same reason, because it takes longer time to reach steady state for a vibration with lower frequency. Additional benefits with the PSD method are described in section 2.3.

In Jiang [3], the term *direct* is defined as follows: "*ground response spectrum is used as input directly without generating any intermediate input such as spectrum-compatible time histories or spectrum-compatible power spectral density functions*". Following this definition, one might question whether Jiang's method or the PSD method can be considered as a purely direct method. In the work performed by Jiang et al [4] [5], they developed statistical relationships for estimating the tRS corresponding to a GRS through the use of a large number of earthquake records. Hence, by adopting these relationships, it is possible to avoid the intermediate step of using spectrum-compatible time histories. However, as mentioned in section 2.2, the statistical relationships presented in [5] to determine the tRS are not applicable for the Swedish earthquake. In the same paper [5], an alternative *amplification ratio method* was proposed for cases when a GRS falls outside the valid coverage range of the statistical relationships. However, also this method showed to be not applicable for the Swedish earthquake. For the interested reader, a MATLAB function is attached to this report (see Appendix A:), where both the statistical relationships and the amplification ratio method from [5] have been implemented. As described in section 2.3, the PSD method requires that a PSD of the GRS is evaluated. Given that the statistical relationships and the amplification ratio method are not universally applicable for all GRS, the effort of determining the PSD is essentially equal. Hence, according to the opinion of the authors of this report, the PSD method should be considered as being as "direct" as the method proposed by Jiang et al. [3] [4] [5].

A general drawback with DSSMs as compared to the time history method is that they normally cannot account for non-linearities since they are based on mode superposition principles. Furthermore, at least for the two DSSMs investigated in this study, the dynamic interaction between the system mounted on the structure and the structure itself cannot be considered. The interaction effects are though only significant if the mass ratio between the system and the structure is not small. In summary, the two investigated DSSMs in this study are judged to be adequately accurate for use in various design situations. One of the most obvious use cases is in preliminary design, where it is normally necessary to investigate several different design alternatives.

5 Conclusions and future work

The FRS obtained using the three different methods considered in this study (one based on time history analysis and two DSSMs) overall show good agreement in shape and acceleration response at the peaks. The results also show that there is a significant scatter at the peaks between the individual FRS obtained from the time history analyses. This highlights the importance of using several sets of acceleration time series followed by averaging of the results when using this method. However, it should be noted that the FRS obtained using either of the two DSSMs mainly fall within the scatter of the time-history based FRS. The two investigated DSSMs in this study can, thus, be concluded to perform well in comparison to the more well-established time series method for evaluation of FRS, and are judged adequate to use in various design situations.

Furthermore, it can be concluded that the required computational time is significantly reduced through the use of DSSMs. In the two presented examples, the analysis time of the time history analyses was roughly 200 times longer than in the eigenfrequency analyses. The use of DSSMs can, thus, in some situations help to significantly speed-up the seismic design of SSCs, e.g. in preliminary design stages where the engineer needs to investigate several different design alternatives. In addition, DSSMs can be an aid in optimization of designs or studying structural weak points for mounting of systems and components in buildings.

As discussed in section 4.3, the definition of direct methods is not completely clear in the literature. For example, according to Jiang [3], DSSMs should not include any intermediate input such as synthetic spectrum-compatible time histories or PSD. However, it was found that the developed statistical relationships and the amplification ratio method for determination of the tRS in Jiang's method are not universally applicable, at least not for the Swedish earthquake. Given this, the effort of determining the PSD in the PSD method and the tRS in Jiang's method is essentially equal. In addition, explicit use of PSDs in what is considered DSSMs has been adopted by other researchers in the literature, see e.g. [33]. Hence, according to the opinion of the authors of this report, the PSD method should be considered as being as direct as Jiang's method.

The results from the examples indicate that the used number of sets of acceleration time series is too small to acquire a generic tRS for the considered design GRS. The same also applies to the average FRS obtained from the time history analyses, where a larger number of sets is necessary to obtain the true average FRS with regard to the design GRS. Hence, to further validate the performance of the DSSMs compared to the time series method, an update of the examples using a larger number of sets of spectrum-compatible time series is necessary. In the work by Jiang et al. [4], at least 30 time series in each direction were used. Another possible approach for evaluating the tRS in Jiang's method is to instead use a spectrum-compatible PSD in a similar fashion as in the PSD method. In future work, it is thus suggested that this alternative approach is to be further investigated.

Concerning the evaluated PSD method in this study, the development is not yet completed. More work is needed, e.g., to find an approach for compensation of

non-stationary response of structures subjected to earthquakes with short strong motion durations. Consequently, the method also needs further verification of its performance. Since the method is still under development and has not been peer-reviewed, no scripts for the method are attached to this report.

Two additional potential features that future development work on the PSD method could result in are worth mentioning. One feature concerns the use of known correlation between the response vibrations given in three orthogonal directions. The eigenmodes of the building is indeed responsible for considerable correlation in the three-dimensional response vibration space, for vibration frequencies around the eigenfrequencies. This output correlation is retained using the PSD-method, just as it is in three-dimensional THA responses. When the building response at a floor location is calculated with the PSD method, you actually get a PSD matrix as output for each response location. The off-diagonal elements of the PSD matrix contain the cross-PSD between output directions, which reveals the correlation between directions (different for different frequencies). As soon as one is leaving the three-dimensional building response for three FRS, calculated from only one vibration projection each, the information about the correlation between projections (or directions) is lost. This feature could be of great importance in qualification of safety equipment, as the qualification then can be made with analysis or testing using true triaxial excitation with correct correlation. Using response spectra for description of seismic requirements is possible also when you want to include vibration response correlation. Correlation between two orthogonal directions can be included through calculation of FRS of several vibration projections, e.g. for every 22.5 degrees, spanned by the two orthogonal directions. Correlation in three dimensions could be illustrated with a half-sphere and a colour mapping of the response amplitude. This three-dimensional format is not possible to use together with a frequency axis, so one will need to use one colour plot per building resonance (FRS peak).

The other potential feature is the incorporation of a generalised coupled PSD-method analysis, in which a fictive SDOF system is attached to the floor location, simulating the effect from a possible resonance in the secondary system. Not considering the coupling effects may result in conservative peaks (higher than the true FRS in a coupled analysis) at building resonance frequencies. If a secondary system has a resonance frequency close to a building resonance, the secondary system will absorb energy from the building vibration like a tuned vibration damper and reduce the building vibration around this frequency. A secondary system with small enough mass, to keep the result on the conservative side, could reduce the FRS peaks and over-testing of equipment in general. Note that you only would need a few fictive SDOF systems, with natural frequencies corresponding to the known building resonance frequencies. It is important to add that this second feature is not unique for the PSD method. The same feature could be implemented with any DSSM or even with THA.

6 References

[1] American Society of Civil Engineers (ASCE), "ASCE 4-98 Seismic Analysis of Safety-Related Nuclear Structures and Commentary," ASCE, USA, 1998.

[2] American Society of Civil Engineers (ASCE), "ASCE 4-16 Seismic Analysis of Safety-Related Nuclear Structures," ASCE, USA, 2017.

[3] W. Jiang, "Direct Method of Generating Floor Respons Spectra," University of Waterloo, Waterloo, Ontario, Canada, 2016.

[4] W. Jiang, B. Li, W.-C. Xie and M. D. Pandey, "Generate floor response spectra: Part 1. Direct spectra-to-spectra method," *Nuclear Engineering and Design,* pp. 525-546, 2015.

[5] B. Li, W. Jiang, W.-C. Xie and M. D. Pandey, "Generate floor response spectra, Part 2: Response spectra for equipment-structure resonance," *Nuclear Engineering and Design,* pp. 547-560, 2015.

[6] C. Lalanne, "Maximax response and fatigue damage spectra - Part I," *Journal of Environmental Scienes,* vol. 27, no. 4, pp. 35-40, 1984.

[7] C. Lalanne, "Maximax response and fatigue damage spectra - Part II," *Journal of Environmental Sciences,* vol. 27, no. 5, pp. 40-44, 1984.

[8] M. P. Singh, "Generation of seismic floor spectra," *Journal of the Engineering Mechanics Division,* vol. 101, no. 5, pp. 593-607, 1975.

[9] M. P. Singh, "Seismic design input for secondary systems," *Journal of the Structural Division,* vol. 106, no. 2, pp. 505-517, 1980.

[10] W. Jiang, Y. Zhou, W.-C. Xie and M. D. Pandey, "Direct Method for Generating Floor Response Spectra considering Soil–Structure Interaction," *Journal of Earthquake Engineering ,* vol. 26, no. 10, pp. 4956-4976, 2020.

[11] R. Wang, W. C. Xie and M. D. Pandey, "Generation of floor response spectra of structures under seismic excitations at multiple supports," *Nuclear Engineering and Design,* vol. 389, p. 111527, 4 2022.

[12] R. Wang, W.-C. Xie and M. D. Pandey, "Generation of floor and tertiary response spectra of structures under seismic excitations at multiple supports," *Earthquake Engineering & Structural Dynamics,* vol. 51, pp. 853-874, 2021.

[13] J. L. Sackman, A. Der Kiureghian and B. Nour-Omid, "Dynamic analysis of light equipment in structures: Modal properties of the combined system," *Journal of Engineering Mechanics,* vol. 109, no. 1, pp. 73-89, 1983.

[14] A. der Kiureghian, J. L. Sackman and B. Nour-Omid, "Dynamic analysis of light equipment in structures: Response to stochastic input," *Journal of Engineering Mechanics,* vol. 109, no. 1, pp. 90-110, 1983.

[15] T. Igusa and A. D. Kiureghian, "Dynamic characterization of two-degreeof-freedom equipment-structure systems," *Journal of Engineering Mechanics,* vol. 111, no. 1, pp. 1-19, 1985.

[16] W.-C. Xie, S.-H. Ni, W. Liu and W. Jiang, Seismic risk analysis of nuclear power plants, Cambridge University Press, 2019.

[17] A. K. Gupta and J. M. Tembulkar, "Dynamic decoupling of secondary systems," *Nuclear Engineering and Design,* vol. 81, no. 3, pp. 359-373, 1984.

[18] A. H. Hadjian and B. Ellison, "Decoupling of Secondary Systems for Seismic Analysis," *Journal of Pressure Vessel Technology,* vol. 108, no. 1, pp. 78-85, 2 1986.

[19] J. M. Biggs and J. M. Roesset, "Seismic analysis of equipment mounted on a massive structure," 1970.

[20] Y. An, "Direct generation of RRS from FRS," 2013.

[21] P. M. Calvi and T. J. Sullivan, "Estimating floor spectra in multiple degree of freedom systems," *Earthquakes and Structures,* vol. 7, no. 1, pp. 17-38, 2014.

[22] T. J. Sullivan, P. M. Calvi and R. Nascimbene, "Towards improved floor spectra estimates for seismic design," *Earthquakes and Structures,* vol. 4, no. 1, pp. 109-132, 2013.

[23] K. Haymes, T. Sullivan and R. Chandramohan, "A practice-oriented method for estimating elastic floor response spectra," *Bulletin of the New Zealand Society for Earthquake Engineering,* vol. 53, no. 3, pp. 116-136, 2020.

[24] R. J. Merino, D. Perrone and A. Filiatrault, "Consistent floor response spectra for performance-based seismic design of nonstructural elements," *Earthquake Engineering and Structural Dynamics,* vol. 49, no. 3, pp. 261-284, 3 2020.

[25] V. Vukobratović and P. Fajfar, "A method for the direct determination of approximate floor response spectra for SDOF inelastic structures," *Bulletin of Earthquake Engineering,* vol. 13, no. 5, pp. 1405-1424, 5 2015.

[26] V. Vukobratović and P. Fajfar, "A method for the direct estimation of floor acceleration spectra for elastic and inelastic MDOF structures," *Earthquake Engineering and Structural Dynamics,* vol. 45, no. 15, pp. 2495-2511, 12 2016.

[27] V. Vukobratović and P. Fajfar, "Code-oriented floor acceleration spectra for building structures," *Bulletin of Earthquake Engineering,* vol. 15, pp. 3013-3026, 2017.

[28] A. Asfura and A. D. Kiureghian, "Floor response spectrum method for seismic analysis of multiply supported secondary systems," *Earthquake Engineering & Structural Dynamics,* vol. 14, no. 2, pp. 245-265, 3 1986.

[29] R. A. Burdisso and M. P. Singh, "Multiply supported secondary systems part I: Response spectrum analysis," *Earthquake Engineering & Structural Dynamics,* vol. 15, no. 1, pp. 53-72, 1 1987.

[30] A. Saudy, "Seismic analysis of multiply-supported MDOF secondary systems," 1992.

[31] S. Rice, "Mathematical Analysis of Random Noise," *The Bell System Technical Journal,* vol. 23, no. 3, pp. 283-332, 1944.

[32] J. Bendat, "Probability Functions for Random Responses: Prediction of Peaks, Fatigue Damage, and Catastrophic Failures," NASA, CR-33, 1964.

[33] R. Donikian, R. Mayes, T. Muraki and L. Jones, "Direct Generation of Seismic Response Spectra," in *4th Canadian Conference on Earthquake Engineering*, Vancouver, 1985.

[34] C. Lalanne, Mechanical vibration and shock - Vol 3: Random Vibration, Paris: Hermes Science Publications, 1999.

[35] Simulia, "Abaqus User's Manual 2022," Simulia, 2022.

[36] C. Rydell, T. Gasch, D. Eriksson and A. Ansell, "Stresses in water filled pools within nuclear facilities subjected to seismic loads," *Nordic Concrete Research,* vol. 51, pp. 43-62, 2014.

[37] SKI, "Characterization of seismic ground motions for probabilistic safety analyses of nuclear facilities in Sweden - Summary Report," SKI Statens kärnkraftsinspektion, SKI Technical Report 92:3, Stockholm, 1992.

[38] C. Rogers, "Suite of ASCE 4-98 compliant time histories to swedish 1e-6 probability of occurance ground free field 5 % spectra," CREA Consultants, 047057151-r001 (Not public), 2016.

[39] SS-EN 1998-1, "Eurocode 8: Design of structures for earthquake resistance - Part 1: General rules, seismic actions and rules for buildings," CEN European Committee for Standardization, Brussels, Belgium, 2004.

Appendix A: MATLAB code – Jiang's DSSM

A zip-archive containing the implementation of Jiang's DSSM in MATLAB is A zip archive containing the implementation of Jiang's DSSM in MATLAB is downloadable from www.energiforsk.se at the same side as this report. The zip-archive also includes all relevant input data for development of the FRS in the two examples presented in sections 3 and 4, together with a main file showing how to use the scripts to calculate the FRS. A short description of all files included in the zip-archive is given in the table below. The acceleration time series used in the examples for the Swedish earthquake are not public, and thus not included in the zip-archive.

Folder	File name	Description
Appendix_A\ jiang_method	corrfrscqc.m	Function to calculate the correlation coefficient matrix using the proposed complete quadratic combination rule FRS-CQC, see example in Figure 2-2.
Appendix_A\ jiang_method	grs2frs.m	Function to calculate floor response spectrum (FRS) from a ground response spectrum (GRS) and corresponding tuning response spectrum (tRS) using Jiang's method.
Appendix_A\ jiang_method	grs2trs.m	Convert ground response spectrum (GRS) to a tuning response spectrum (tRS) using the statistical relationships or the amplification ratio method from reference [5].
Appendix_A\ jiang_method	th2trs.m	Function to calculate tuning response spectrum from an acceleration time history/series using Eq. (2-9).
Appendix_A\ examples	abaqus_dat_reader.m	Function to read output data from Abaqus .dat files. Function from MATLAB Central written by Michael Jandron, Brown University, US.
Appendix_A\ examples	main_example.m	Main file to evaluate the FRS in the two examples using the functions in folder Appendix_A\jiang_method.
Appendix_A\ examples	tRS_H_mean.mat tRS_H1_mean.mat tRS_H2_mean.mat	MATLAB data files containing the average tRS in horizontal directions used in the examples: H: average of all ten horizontal time series H1: average of the five horizontal time series used in direction H1 H2: average of the five horizontal time series used in direction H2
Appendix_A\ examples	tRS_V_mean.mat	MATLAB data file containing the average tRS in vertical direction used in the examples.

Folder	File name	Description
Appendix_A\ examples\ example 1	Simple_containment_EigenFreq.inp	Abaqus input file for the eigenfrequency analysis in Example 1
Appendix_A\ examples\ example 1	Simple_containment_TransModal.inp	Abaqus input file for the THA in Example 1
Appendix_A\ examples\ example_1\ freq_results	Mode_shape_*.txt	Text files containing the mode shapes at the selected nodes in Example 1.
Appendix_A\ examples\ example_1\ freq_results	Simple_containment_EigenFreq.dat	Abaqus .dat file containing results from the eigenfrequency analysis in Example 1.
Appendix_A\ examples\ example_1\ result_plots	FRS_*.jpg	Plots of FRS at the selected nodes in Example 1.
Appendix_A\ examples\ example_1\ th_results	Acc_TH_set_X_*.txt	Text files containing the acceleration time histories at the selected evaluation nodes in Example 1 for set X of ground acceleration time series (five sets in total).
Appendix_A\ examples\ example_1\ th_results	frsContainmentTimeHistTM.mat	MATLAB data file containing the calculated FRS at the selected nodes from the time history analyses in Example 1.
Appendix_A\ examples\ example 2	Building_DSSM_eigen.inp	Abaqus input file for the eigenfrequency analysis in Example 2
Appendix_A\ examples\ example 2	Building_DSSM_TM.inp	Abaqus input file for the THA in Example 2
Appendix_A\ examples\ example_2\ freq_results	Mode_shape_BUILDING-1_*.txt	Text files containing the mode shapes at the selected nodes in Example 2.
Appendix_A\ examples\ example_2\ freq_results	Building_DSSM_eigen.dat	Abaqus .dat file containing results from the eigenfrequency analysis in Example 2.
Appendix_A\ examples\ example_2\ result_plots	FRS_*.jpg	Plots of FRS at the selected nodes in Example 2.
Appendix_A\ examples\ example_2\ th_results	Acc_TH_set_X_BUILDING-1_*.txt	Text files containing the acceleration time histories at the selected evaluation nodes in Example 2 for set X of ground acceleration time series (five sets in total).

Folder	File name	Description
Appendix_A\ examples\ example_2\ th_results	frsBuildingTimeHistTM.mat	MATLAB data file containing the calculated FRS at the selected nodes from the time history analyses in Example 2.

DIRECT SPECTRA-TO-SPECTRA METHODS

The obtained floor response spectra (FRS) using the two studied direct spectra-to-spectra methods (DSSM) and the time series method show an overall good agreement in shape and acceleration response at the peaks. The results also show that there is a significant scatter at the peaks between the individual FRS obtained from the time history analyses. These results highlight the importance of using several sets of acceleration time series followed by averaging of the results when using this method. However, the FRS obtained using either of the two DSSMs mainly fall within the scatter of the time-history based FRS. The two investigated DSSMs in this study can, thus, be concluded to perform well in comparison to the more well-established time series method for evaluation of FRS, and are judged adequate to use in various design situations.

A new step in energy research

The research company Energiforsk initiates, coordinates, and conducts energy research and analyses, as well as communicates knowledge in favor of a robust and sustainable energy system. We are a politically neutral limited company that reinvests our profit in more research. Our owners are industry organisations Swedenergy and the Swedish Gas Association, the Swedish TSO Svenska kraftnät, and the gas and energy company Nordion Energi.

Energiforsk